Since January 2020 Elsevier has created a COVID-19 resource centre with free information in English and Mandarin on the novel coronavirus COVID-19. The COVID-19 resource centre is hosted on Elsevier Connect, the company's public news and information website.

Journal Pre-proof

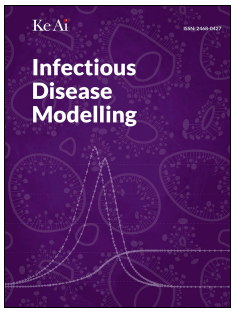

The effect of non-pharmaceutical interventions on COVID-19 outcomes: A heterogeneous age-related generalisation of the SEIR model

Jorge M. Mendes, Pedro S. Coelho

PII: S2468-0427(23)00044-1

DOI: https://doi.org/10.1016/j.idm.2023.05.009

Reference: IDM 383

To appear in: *Infectious Disease Modelling*

Received Date: 21 September 2022

Revised Date: 26 May 2023

Accepted Date: 29 May 2023

Please cite this article as: Mendes J.M. & Coelho P.S., The effect of non-pharmaceutical interventions on COVID-19 outcomes: A heterogeneous age-related generalisation of the SEIR model, *Infectious Disease Modelling* (2023), doi: https://doi.org/10.1016/j.idm.2023.05.009.

Title: The effect of Non-Pharmaceutical Interventions on COVID-19 outcomes: a heterogeneous age-related generalisation of the SEIR model

Jorge M. Mendes (corresponding author)

NOVA Information Management School (NOVAIMS)

Universidade Nova de Lisboa

Campus de Campolide, 1070-312 Lisbon, Portugal

NOVA Cairo at The Knowledge Hub

New Admnistrative Capital, Cairo, Egypt

jmm@novaims.unl.pt

Pedro S. Coelho

NOVA Information Management School (NOVAIMS)

Universidade Nova de Lisboa

Campus de Campolide, 1070-312 Lisbon, Portugal

psc@novaims.unl.pt

The effect of Non-Pharmaceutical Interventions on COVID-19 outcomes: a heterogeneous age-related generalisation of the SEIR model*

Jorge M. Mendes
NOVA Information Management School (NOVAIMS)
Universidade Nova de Lisboa
Campus de Campolide, 1070-312 Lisbon, Portugal
NOVA Cairo at The Knowledge Hub Universities
New Admnistrative Capital, Cairo, Egypt

Pedro S. Coelho
NOVA Information Management School (NOVAIMS)
Universidade Nova de Lisboa
Campus de Campolide, 1070-312 Lisbon, Portugal

First version: February 28, 2022
This version: May 26, 2023

Abstract

Successive generalisations of the basic SEIR model have been proposed to accommodate the different needs of the organisations handling the SARS-CoV-2 epidemic and the assessment of the public health measures adopted and named under the common umbrella of Non-Pharmaceutical Interventions (NPIs). So far, these generalisations have not been able to assess the ability of these measures to avoid infection by the SARS-CoV-2 and thus their contribution to contain the spread of the disease. This work proposes a new generalisation of SEIR model and includes a heterogeneous and age-related generation of infections that depends both on a probability that a contact generates the transmission of the disease and a contact rate. The results show (1) thanks to the universal wearing of facial coverings, the probability that a contact provokes the transmission of the disease was reduced by at least 50% and (2) the impact of the other NPI is so significant that otherwise Portugal would have gone into a non-sustainable situation of having 80% of its population infected in the first 300 days of the pandemic. This situation would have led to a number of deaths almost twenty times higher than the number that was actually recorded by December 26^{th}, 2020. Moreover, the results suggest that even if the requirement of universal wearing of

*Corresponding address: jmm@novaims.unl.pt

facial coverings was adopted sooner jointly with closing workplaces and resorting to teleworking would have postponed the peak of the incidence, altought the epidemic path would have result in a number of infections hardly managed by the National Health System. Complementary, results confirm that (3) the health authorities adopted a conservative approach on the criteria to consider an infected individual not infective any longer; and (4) the most effective NPIs and stringency levels either impacting on self-protection against infection or reducing the contacts that would eventually result in infection are, in decreasing order of importance, the use of *Facial coverings*, *Workplace closing* and *Stay at home requirements*.

Contents

1 Introduction

In December 2019, a new coronavirus named Severe Acute Respiratory Syndrome-Coronavirus-2 (SARS-CoV-2), causing severe acute respiratory disease emerged in the region of Wuhan, China (Zhu et al. (2020) and Chan et al. (2020)). SARS-CoV-2 is an acute respiratory infectious disease that spreads through the respiratory tract by droplets, respiratory secretions, person-to-person contact and objects or materials which are likely to carry infection, such as clothes, utensils, and furniture (Chen (2020), Wang et al. (2020) and Rosa et al. (2020)).

At the time of writing this introduction almost all European countries have been through at least five "waves", but the effect induced by the high vaccination coverage started to appear (Gozzi, Bajardi, and Perra (2021)). Consequently, many countries began to ease some of the heavy measures in force and the mandatory use of face masks was even under judicious evaluation. Indeed, in the fight against this coronavirus and the absence of a vaccine or treatment, the international community was more interested in putting in force measures to control the spread of the virus and/or mitigate it. The extent (stringency and duration) which these measures were adopted depends either on the epidemiological situation, the population being targeted or the governments sensitivity to their economic impact. Furthermore, the actions taken potentially mitigate the spread of infection by the SARS-CoV-2 and contribute to preserving the health of citizens (Ferguson et al. (2020), Nunan and Brassey (2020)).

It is possible to organise the spectra of all mitigation measures taken under a common umbrella named Non-Pharmaceutical Interventions (NPIs), that is, any public health measures that aim to prevent and/or control infection transmission in the community. During the period when there was no effective and safe vaccine to protect those at risk of severe COVID-19, NPIs were seen as the most effective public health instruments against COVID-19. The European Centre for Disease Prevention and Control (ECDC) guidelines detail available options for NPIs in various epidemiological scenarios, assess the evidence for their effectiveness and address implementation issues, including potential barriers and facilitators (European Centre for Disease Prevention and Control (2020)). According to the ECDC, NPIs can be classified into three levels of implementation: individual, environmental and population levels. In parallel to these guidelines, the ECDC keeps tracks of selected national public NPIs presented in the weekly COVID-19 country overviews report.

The best available scientific evidence is required to design effective NPIs and disseminate the knowledge to help public officials assess the potential benefits and costs of NPIs to contain COVID-19 outbreaks, as it is to expect that different measures will also present different levels of cost-effectiveness. Therefore, it is essential to describe how different countries implemented NPIs, and at what point of the epidemic. It is also necessary to explore how those NPIs have impacted the number of cases, the mortality, and the capacity of health care facilities to deliver healthcare services.

As early as December 2022, a search of published scientific material on **"Covid-19"** and

NPIs (searched as *non-pharmacologial interventions*, *non-pharmacological interventions* or *non-pharmaceutical*) on *ISI Web of Knowledge* returned 452 entries. A refinement based on scientific areas, publishing outlets and topics addressed restricted the number of publications, yet far above 200. A read over their abstracts unveiled a broad spectrum of used methodologies, although their conclusions were coincident to some extent. It is not the authors' purpose to perform a systematic literature review here, especially when others have been successfully doing so. Therefore, regarding the different methodologies used to perform the NPIs assessment, we refer to the outstanding systematic review by Banholzer et al. (2022). In this work, the authors systematically review the literature on assessing the effectiveness of non-pharmaceutical interventions between January 1, 2020 and January 12, 2021, using a total of 248 publications. Although despite the substantial variation in methodologies with respect to study setting, outcome, intervention, methodological approach, and effectiveness assessment, which prevents comparability among studies, the heterogeneity in the used methodologies may be desirable to assess the robustness of results, the study points out to shortcomings of existing studies and make recommendations for the design of future ones. Regarding the empirical studies and their results about the effectiveness of NPIs we refer to the excellent review carried out by Mendez-Brito, Bcheraoui, and Pozo-Martin (2021). In this review the authors followed the a systematic methodology (PRISMA) (Moher et al. (2009)) to search for published literature and preprints, respectively, available in English from January 1, 2020 to the beginning of March 2021. The authors rank the NPIs according to their effectiveness in reducing reproduction number, infection growth rate, and other incidence-related measurements. Overall, school closing was the most effective measure in reducing the number of cases. As they point out, several authors report a mean reproduction number reduction after the closures of educational facilities. Indeed, after the closure of schools and universities Brauner et al. (2021) estimated a mean reproduction number reduction of 39%. In turn, Haug et al. (2020) estimated a reduction of 73% after the school closing. Workplace closing to at greater extent and business or venue closing and public event bans to a less one are considered the most effective in reducing cases.

Other NPIs such as lockdowns, movement limitations through national or international travel restrictions, social gathering bans ranging from 10 people to mass gathering bans, social distancing, public information campaigns and mask-wearing requirements are reported as a group of intermediate effectiveness yet still important.

Several authors seem to have found no evidence of the effectiveness of other NPIs like public transport closure, testing and contact tracing strategies and quarantining or isolation of individuals. Also, limited work and evidence indicate that stringency may play an important role when adopting a NPI (Liu et al. (2021)). Finally, the specific topic of face masks has also been addressed, suggesting that the broad adoption of even relatively ineffective face masks may meaningfully reduce community transmission of COVID-19. However, several of these results are contradictory, limited in outcomes analysed (e.g. limited to the reproduction number) and partial in the sense that they do not address the combined effect of different

NPIs and, in particular, the role of face masks in the presence of other NPIs (Eikenberry et al. (2020)).

Although almost all the conclusions of the empirical studies have pointed out to coincident effects of some NPIs regarding their ability to mitigate or stop disease spread, several factors have also been reported to be of critical importance for NPIs effective impact (e.g. Barbarossa and Fuhrmann (2021)). These factors affect the population's compliance to adopting NPIs, which can even be graded in concern, government performance's perception or agreement and compliance (e.g.} Santos et al. (2022)). Their nature ranges from demographic, social and psychological (e.g. Seale et al. (2020), Shittu et al. (2022), Hengartner, Waller, and Wyl (2022), Downing et al. (2022) and Sopory, Novak, and Noyes (2022)).

As Kretzschmar et al. (2022) points out, mathematical modelling and statistical inference provide a framework to evaluate different non-pharmaceutical and pharmaceutical interventions to control epidemics. However, addressing the challenges in modelling the health, economic and political aspects of interventions need a wide variety of interdisciplinary expertise and cross-collaboration between scientists and policymakers, combining mathematical knowledge with biological and social insights, including health economics and communication skills.

All things considered, there are still crucial knowledge gaps on the effectiveness of different interventions to adequately justify the preparation, implementation, or cancellation of various NPIs. In addition, governments across the World need evidence as to the combination and timings of each potential NPI, which remains lacking (e.g.@Patino2020). Despite this discussion, the ultimate goal of the different NPIs referred to above is to reduce the number of contacts between humans or lower the probability of transmission, especially between the most exposed to infection and those who exhibit particular vulnerabilities, and therefore mitigate and contain the spread of the infection. The reduction in human contacts is hard to quantify, but proxy variables exist that aid the investigation of NPIs effects, Google (https://google.com/covid19/mobility/) or Apple mobility (https://covid19.apple.com/mobility) data are two examples of those proxies.

The motivation of this work is anchored on the current lack of knowledge about the effectiveness of different NPIs. Additionally, the authors aim to provide a comprehensive framework to assess the effect of different NPIs adopted during the pandemic. Indeed, using an extension of the widely known compartmental model, the ***S****usceptible-****E****xposed-****I****nfected-****R****emoved* (SEIR) model, the authors set up a methodology to assess the direct effects NPIs on population mobility and their indirect impacts on the spread of the infection. Additionally, simulations are performed to assess what would have happened if those NPIs or only a subset of them were adopted. Therefore, its purpose is to understand how NPIs have affected the mobility of citizens and the probability of disease transmission. These data are subsequently used to mimic how the contact rate evolved and how it impacts the daily generation of confirmed COVID-19 cases. A set of simulations also aims to compare the effects of different NPIs on the most relevant outcomes of the epidemic, namely the accumulated number of infections

and deaths. All this is performed by proposing a generalisation of the SEIR model that accommodates heterogeneity between age-groups and a Bayesian estimation framework. A time-varying contact-mobility matrix is also proposed as an input for the estimation framework.

This work is organised as follows. Section 1 introduces the research problem and the overall research objective. Section 2.1 describes the data used, namely the COVID-19 daily epidemic data (Section 2.1.1), the age-group specific contact matrices (Section 2.1.2) and the NPIs data (Section 2.1.3). Section 2.2 presents the SIR model, its extension to accommodate the necessary period of virus incubation, as known as SEIR model (Section 2.2.1), and its generalisation to account for COVID-19 infection heterogeneity across different age groups due to age-dependent contact rates and mobility levels temporal paths (section 2.2.2). These age-dependent contact rates and mobility levels temporal paths are incorporated into the model's time-varying contact-mobility matrix obtained as described in Section 2.2.3. These section finishes with a full description of the Bayesian framework conceptual model and it estimation details (Section 2.2.4). Section 3 presents the main results and, lastly, Section 4 discusses the main conclusions as well as their implications in epidemiology policy-making.

2 Materials and methods

2.1 Data

2.1.1 Data on COVID-19 pandemic

Epidemic data were collected from the Data Science for Social Good (DSSG (2022)) relative to Portugal. The dataset used contains the data released by the *Direção-Geral de Saúde* (Directorate-General of Health, DGS), the Portuguese health authority. Since the beginning of the pandemic, DGS releases daily data on its course. The key released variables used for modelling purposes as explained below are age-stratified (in decennial groups, 0-9, 10-19, 20-29, 30-39, 40-49, 50-59, 60-69 and 70 and more years old) number of confirmed cases number of deaths, and number of recovered cases (not age-stratified).

The period of analysis ranges from March 3^{rd} 2020 to December 26^{th} 2020. It corresponds to a period where several NPIs were implemented (ranging from simple recommendations to law enforcement) and matches the period when vaccines were not yet available. The course of the epidemic over this period is shown in Figure 1.

Figure 1 illustrates the occurrence of two distinct waves. The first occurred between mid-March and the beginning of May 2020 and the second commenced in late August until late December 2020. Yet out of the current time frame, a third wave occurred in January 2021, leading to the highest spikes Portugal had experienced ever.

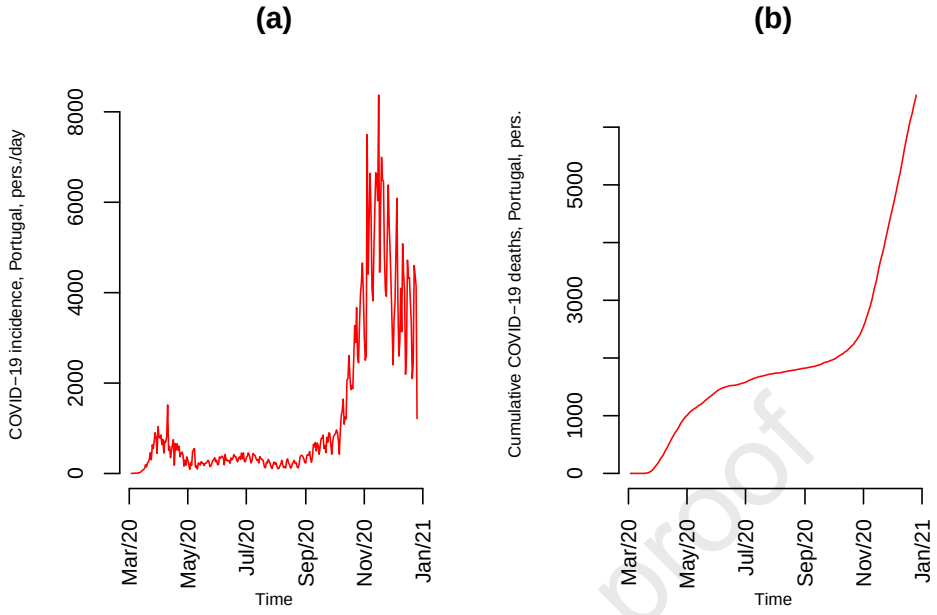

Figure 1: Course of the COVID-19 epidemic in Portugal. (a) Daily infected cases. (b) Deaths (cumulative)

2.1.2 Age-group contact matrix

Quantifying what entails a *contact* that is sufficient to transmit a disease can be extraordinary difficult, especially with a disease like COVID-19 that can be spread with even causal incidental contact with a infected person. Several comprehensive works have been made throughout the last fifteen years to quantify contacts (e.g. Mossong (2008), Prem, Cook, and Jit (2017), Arregui et al. (2018)). Here, due to nonexistence of infection data by location, we shall use the contact matrix *for all locations* estimated by Prem et al. (2017) for Portugal. As Chikina and Pegden (2020) points out, the matrices provided by Prem et al. (2017) are asymmetric, because his empirical work information collected regards contacts experienced with other that might not be part of the target population and matrices correspond to absolute frequencies of interactions between age groups, rather than frequencies relative to the sizes of the age groups. The age-structured model used here already account for the susceptible population which belongs to each age group, thus we processed the contact matrices as Chikina and Pegden (2020) describes:

1. To correct for the second source of asymmetry by dividing each column by the proportion of the population in the corresponding age group;

2. To correct the first source of asymmetry by averaging out the pairs of elements reflected across the diagonal.

The age-group contact matrix $\mathbf{C}$ is a $G \times G$ matrix representing the average daily number of contacts between each pair of age-groups, where G here denotes the number of age-groups considered. We denote the matrix entry $[C_{ij}]$, $i, j = 1, \ldots, G$ as the average daily number of contacts the people in the age-group i (matrix row index) have with people in age-group j (matrix column index).

Prem et al. (2017) reports matrices for 16 quinquennial age-groups ([0,4], [5,9],..., [70,74], [75,∞]). As the COVID-19 related data is only available at decennial age-groups, prior to the asymmetry correction described above, were obtained by aggregating quiquennial age-groups to decennial ones ([0,9]=[0,4]+[5,9], [10,19]=[10,14]+[15,19],..., [70,...]=[70,74]+[75,∞]), taking in consideration their relative demographic weight. The used matrix is represented in Figure A4(a), where the cell figures represent the average number of daily contacts of people in the age-group i (row index, $i = 1, 2, ..., 8$) with people in the age-group j (column index, $j = 1, 2, ..., 8$), and the 5-tone cyan scale denotes their intensity. Notice that there is a strong tendency for people to prefer contacts with their peers. Also, there is evidence of the child/parent and grandchild/grandparent interactions.

2.1.3 Non-pharmaceutical interventions data

Information on NPIs was mainly obtained from the Oxford COVID-19 Government Response Tracker (OxCGRT) (https://www.bsg.ox.ac.uk/research/research-projects/covid-19-government-response-tracker) which collects systematic information on policy measures that governments have taken to tackle COVID-19. The different policy responses have been tracked since 1 January 2020, covering more than 180 countries, coded into 21 indicators, including a miscellaneous notes field organised into five groups, containment and closure policies, economic policies, health system policies, vaccination policies and miscellaneous policies. These policies are recorded on a scale to reflect the extent and stringency of government action. For more detailed information please refer to Table A1 in Appendix. The selection of NPI indicators used in this work, along with their time extent and stringency, is represented in Figure 2.

The stringency scale of NPIs represented in Figure 2 differs across the eight categories (cf. Table A1 in Appendix). However its possible to group them into three groups. A first group of NPIs whose stringency scale ranges from 0 to 4, which is the case of *Resctriction on gatherings*, *Facial coverings* and *International travelers controls*; a second group whose scale ranges from 0 to 3, which the case of *Stay at home requirements* (lockdown), *Workplace closing* and *School closing*, and, finally, a group composed of *Close public transport* and *Cancel public events* whose scale ranges from 0 to 2. In any case the "0" denotes absence of the measures and the scale maximum denotes the most higher stringency. The colour scale used in Figure 2 uses no colour (white) for scale value "0" and "the darker cyan tone" for the most stringest case. The intermediate stringency levels are represented by lighter cyan tones. Be aware that in Portugal some intermediate stringency levels of some measure do not exist,

therefore aggregation was done for modelling purposes (cf. Table A1 in Appendix).

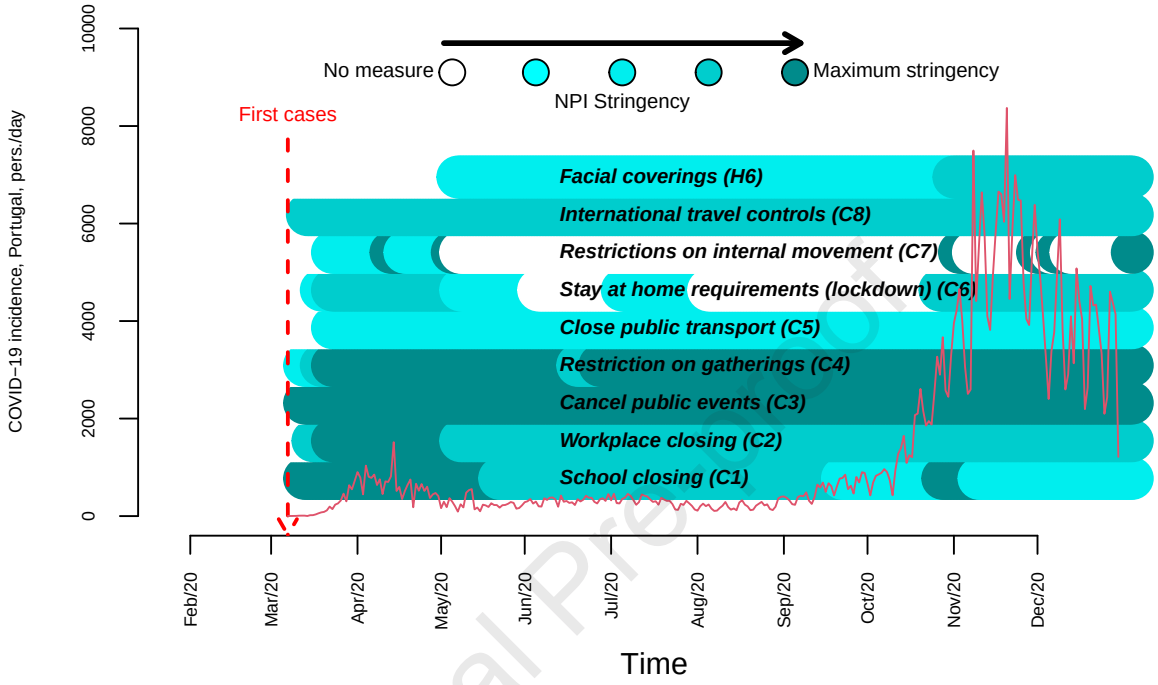

Figure 2: Daily infections and Non-Pharmaceutical Interventions data in Portugal.

Figure 2 shows the NPI and the curve of daily cases in the analysis timeline. During the SARS-CoV-2 epidemic in Portugal four distinct periods can be distinguished. The first one, between the beginning of the epidemic and the declaration of a *state of emergency*, the first hard lockdown control measures (on March 18^{th} 2020). The second one, between March 18^{th}, 2020, and the declaration of the *situation of calamity* when the lockdown measures started easing (May 4^{th}, 2020). A third period from May 4^{th} onwards and until August 18^{th}, corresponding to the traditional Portuguese holidays period and the beginning of the school year and finally, from August 18^{th} onwards.

For modelling purposes, it is observable that the discriminating levels (cf. Table A1 in Appendix) of some NPIs might raise collinearity issues for model estimation. Section 2.2.4 explains the aggregation of some stringency levels and justifies the exclusion of NPIs from the analysis.

2.2 Methods

2.2.1 The SIR and SEIR models

Much work has been done so far on the course of the COVID-19 outbreak using the so-called compartmental models (Abou-Ismail (2020), Ndaïrou et al. (2020), Wang et al. (2020)). The origin of compartmental models dates back to the early 20th century with the seminal work of Kermack and McKendrick (in 1927) (Kermack and McKendrick (1927)). Compartmental models simplify the mathematical modelling of infectious diseases. The population is assigned to compartments and may progress between compartments. Compartmental order usually shows flow patterns between the compartments; for example, SIS means susceptible, infectious, and then susceptible again (Hethcote (2000)). The models are most often run with ordinary differential equations (which are deterministic). Still, they can also be used with a stochastic framework (Hethcote (2000)).

Compartmental models allow predicting how a disease spreads through the total number infected, the duration of an epidemic, and infection reproductive number (R_0), among other important epidemic course parameters. Moreover, such models could potentially be used as a framework to show how different public health interventions (e.g. vaccination, limited social contacts, lockdown) may affect the outcome of the epidemic.

The basic compartmental model is the SIR model (Kermack and McKendrick (1927)). Nonetheless, it still captures the main properties of an epidemic (Anderson (1991), Kaye (1993)), and it has been widely used in epidemic modeling studies. The SIR model comprises three compartments: S for the number of susceptible, I for the number of infectious, and R for the number of removed (recovered, deceased, or immune) individuals at a particular time (Figure 3(a)). This model assumes incidence grows exponentially, which is not in agreement with the observed epidemic course, as the measures adopted by public health authorities at different moments, as well as the change in human behaviours tend to flatten the parabolic incidence curve. Therefore, its predictive value for infectious diseases that are transmitted from humans to humans, without any change in the constant transmission rate is of limited usefulness.

To represent that the number of susceptible, infectious and removed individuals may vary over time (even if the total population size remains constant) a time index, t, might be added: $S(t)$, $I(t)$ and $R(t)$.

For infections with the characteristics of COVID-19, there is a significant incubation period during which individuals have been infected but are not yet infectious themselves (European Center for Disease Prevention and Control (2020), Tang et al. (2020), Lauer et al. (2020), Zhou et al. (2020)). During this period the individual is in compartment $E(t)$ (for exposed), resulting in the so-called SEIR model. Moreover, many authors (Godio, Pace, and Vergnano (2020), Wang et al. (2020), Mendes and Coelho (2021)) have been proposing generalisations of this basic SEIR model by splitting the compartment, R into two compartments, one to

account for the infected people that genuinely recover from the disease, R, and a second one to account for the mortality induced by the infection, D. For a specific disease within a particular population, these functions may be worked out to predict possible outbreaks and bring them under control.

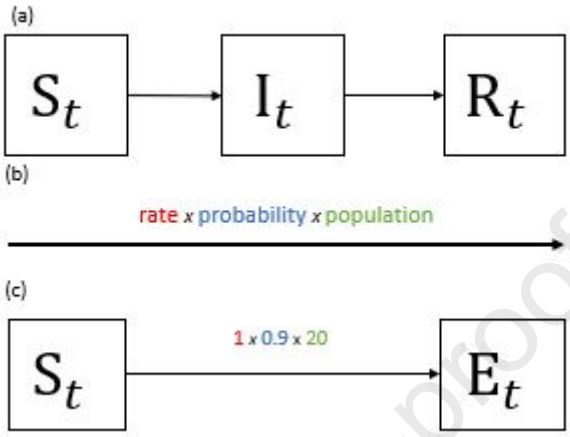

Figure 3: The SIR and SEIR models. (a) SIR model. (b) Generic transitions between compartments.

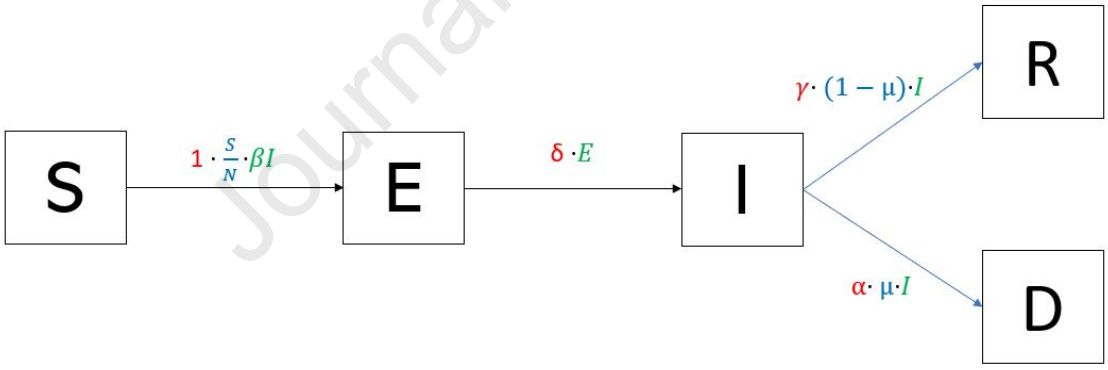

Figure 4: The SEIRD model.

In Figures 3 and 4 the boxes represent the compartments (or states) and arrows represent transitions from one compartment to another. $S(t)$ is the number of people susceptible at time t, $E(t)$ is the number of people exposed to the infection at time t (people that become infected but not infectious), $I(t)$ is the number of infective people infected at time t, $R(t)$ is the number of people recovered at time t and $D(t)$ is the number of deceased at time t. Transitions from one compartment to another usually follow the framework represented in Figure 3(b). The *rate* describes how long the transition takes, *population* is the group of individuals that this transition applies to, and *probability* is the probability of the transition taking place for an individual.

The full SEIRD model is depicted in Figure 4. The transitions from E to I and from I to R or D occur with the probability being 1 (everyone infected will certainly become infectious), $1-\mu\prime$ (a share of $1-\mu\prime$ infectious people will recover, usually expressed in "%") and $\mu\prime$ (a share of $\mu\prime$ infectious people will die, usually expressed in "%") and the population is E and I, respectively. Here δ is the rate at which infected people become infectious (days^{-1}). The recovery rate is $\gamma\prime$ (expressed in days^{-1}), $\mu\prime$ is the fatality share (usually expressed in "%"), and α is the rate at which people die (expressed in days^{-1}). In general, it is not possible to identify parameters α, $\mu\prime$ and $\gamma\prime$, therefore a simplification is assumed hereafter, that is, $\gamma = \gamma\prime \times (1-\mu\prime)$ (expressed in days^{-1}) and $\mu = \alpha \times \mu\prime$ (expressed in days^{-1}), where $\gamma\prime$ and $\mu\prime$ represent the latent, non-identifiable, crude recovery and fatality share, respectively.

The following differential equations describe transitions of the SEIRD model:

$$\begin{aligned}
\frac{\partial S(t)}{\partial t} &= -\beta S(t)\frac{I(t)}{N} \\
\frac{\partial E(t)}{\partial t} &= \beta S(t)\frac{I(t)}{N} - \delta E(t) \\
\frac{\partial I(t)}{\partial t} &= \delta E(t) - \gamma I(t) - \mu I(t) \\
\frac{\partial R(t)}{\partial t} &= \gamma I(t) \\
\frac{\partial D(t)}{\partial t} &= \mu I(t) \\
N &= S(t) + E(t) + I(t) + R(t) + D(t)
\end{aligned} \tag{1}$$

The parameter β denotes the transmission rate, that is, the expected number of people an infected person infects per day and is the result of the **contact rate** c - the number of people an average person enters into contact with each day - and the **probability that a contact provokes the transmission of the disease**, ψ). Usually no data is available allowing estimation of ψ and c separately; hence, β is directly estimated. However, either ψ might change over time as a result, for example, of new virus variants or c is affected by changes in individual behaviour and NPIs put in place by the governments. Here we propose to replace c with age-structured contact matrices describing the rate of contact between each pair of ages. More specifically, we consider an age-structured model as used by (Ram and Schaposnik (2021)) in which we compute the age distribution of each compartment in decennial age-groups (0-9,10-19,. . . ,60-60, 70+), incorporating age-group-dependent contact-mobility matrix describing the rate of contact between each pair of age-groups. In doing so, we aim to capture the heterogeneous effect of COVID-19 across different ages as well as the impact of the NPI both across different age-groups and age-specific daily environments.

2.2.2 The age-structured SEIRD model

In the following the rationale underlying the age-structured SIR model is presented. As the permanent knowledge of the deaths generated by COVID-19 is of crucial importance to

monitoring the pandemic's effects we have split the previous *R*emoved compartment into *R*ecovered and *D*eath compartments, allowing us to monitor the recovering rate and the age-specific fatality rates. The system of ordinary differential equations in (1) is replaced by a system of age-stratified ordinary differential equations here:

$$\begin{aligned}
\frac{\partial S_i(t)}{\partial t} &= -\psi(t) S_i(t) \sum_{j=1}^{G} M_{ij}(t) \frac{I_j(t)}{N_j} \\
\frac{\partial E^i(t)}{\partial t} &= \psi(t) S_i(t) \sum_{j=1}^{G} M_{ij}(t) \frac{I_j(t)}{N_j} - \delta E_i(t) \\
\frac{\partial I_i(t)}{\partial t} &= \delta E_i(t) - \gamma_i I_i(t) - \mu_i I_i(t) \\
\frac{\partial R_i(t)}{\partial t} &= \gamma_i I_i(t) \\
\frac{\partial D_i(t)}{\partial t} &= \mu_i I_i(t) \\
N_i &= S_i(t) + E_i(t) + I_i(t) + R_i(t) + D_i(t) \\
N &= S(t) + E(t) + I(t) + R(t) + D(t) \\
E(t) &= \sum_{i=1}^{G} E_i(t),\ I(t) = \sum_{i=1}^{G} I_i(t),\ R(t) = \sum_{i=1}^{G} R_i(t),\ D(t) = \sum_{i=1}^{G} D_i(t).
\end{aligned} \tag{2}$$

where i and j, $i, j = 1, ..., G$ are the age groups, $\psi(t)$ is the probability of transmission given a contact, δ is the rate at which an infectious individual becomes infective, γ_i is the rate of recovery, μ_i is the age-group specific fatality rate, and N_i is the population size of age group g.

The parameter δ is the inverse of the average incubation period and governs the lag between having undergone an infectious contact and becoming infective. It is generally considered fixed because it depends mainly on the infectious agent's characteristics. Here we use the value 1/5.1 (Linton et al. (2020), Li et al. (2020)).

The parameter γ_i is the recovery rate for infected people. It corresponds to the inverse of the average time required for an active case to recovers. It provides precious information about how fast the people may recover from the disease (in days, in general). We believe that γ_i is dependent on the individual health status which subsequently highly dependent on the individual age, but relatively constant in time. However, in this work, due to the lack of reliable empirical information on the daily recovered patients, we consider γ to be fixed across all age-groups and equal to 1/14 (1/days) (Tang et al. (2020)). The practitioner that needs to estimate this parameter might set a gamma prior, Ga(1, 1/14), that corresponds to a mean recovery period of 14 days and accounts for some uncertainty and variability in the patients recovery time. As discussed by Mendes and Coelho (2021), other formulations are possible to account for temporal variation as well.

The parameter μ_i is the fatality rate and provides information simultaneously on the proportion of infected individuals who, unfortunately, die and the time undergone infective as before death. It depends, indeed, on the patients' resilience, the severity of the disease and the health system capability to treat people over time (e.g., with the introduction of a new therapy). However, due to the short period under analysis we do not consider μ_i to be time-dependent.

The probability of transmission of the disease given a contact $\psi(t)$ depends mainly on the virus spreading ability which might be affected by self-protection measures. Whilst the former is highly related to the relative importance of the virus variants in circulation in a community, the latter is associated with the general level of use of facial covering devices. Here, due to the relatively short period in analysis which was not particularly affected by diverse virus variants, but reliable information on the use of facial coverings is available, we model $\psi(t)$ as a step function distinguishing three distinct periods i.e., before any facial covering has even been recommended (cf. stringency "0" according to the OxCGRT scale), the period when they were *required in some specified shared/public spaces outside the home with other people present, or some situations when social distancing not possible* (cf. stringency "2" according to the OxCGRT scale) and the period when they were *required in all shared/public spaces outside the home with other people present or all situations when social distancing not possible* (cf. stringency "3" accoding to the OxCGRT scale). In the Bayesian framework proposed below all the parameters associated with these binary variables are considered stochastic with associated prior distributions.

The contact-mobility matrix entries, $\mathbf{M}(t) = [M_{ij}(t)]_{i,j=1}^{G}$, defined in (5) are considered stochastic as described in Section 2.2.4. The simulation of the course of the epidemic assuming no NPIs were adopted is done assuming the contact-mobility matrix is constant over time, as described in Section 2.2.3, in (6).

For modelling performed hereafter, one uses a discrete-time approximation to the stochastic continuous-time SEIRD model defined in (2). Consider a time interval $(t, t+h)$, where h represents the length between the time points at which measurements are taken, here $h = 1$ day. Let $dE_i(t)$ denote the daily number of susceptible individuals who become infected, $dI_i(t)$ the daily number of infected individuals who become infectious, $dR_i(t)$ the daily number of infectious cases who recover, and $dD_i(t)$ the daily number of infectious cases who decease in age group i, $i = 1, ..., G$, $t = 1, ..., T$. Given initial conditions $S_i(0) = s_i(0)$, $E_i(0) = e_i(0)$, $I_i(0) = i_i(0)$, $R_i(0) = 0$ and $D_i(0) = 0$, and the population size N, the discretised stochastic

SEIRD model is specified by:

$$
\begin{aligned}
S^g_{t+1} &= S_i(t) - dE_i(t),\ g = 1, ..., G, t = 0, ..., T-1 \\
E^g_{t+1} &= E_i(t) + dE_i(t) - dI_i(t),\ g = 1, ..., G, t = 0, ..., T-1 \\
I^g_{t+1} &= I_i(t) + dI_i(t) - dR_i(t) - dD_i(t),\ g = 1, ..., G, t = 0, ..., T-1 \\
R^g_{t+1} &= R_i(t) + dR_i(t),\ g = 1, ..., G, t = 0, ..., T-1 \\
D^g_{t+1} &= D_i(t) + dD_i(t),\ g = 1, ..., G, t = 0, ..., T-1
\end{aligned}
$$

$$
\begin{aligned}
dE_i(t) &= \psi(t) S_i(t-1) \sum_{j=1}^{G} M_{ij}(t) \frac{I_j(t-1)}{N_j},\ i = 1, ..., G, t = 1, ..., T \\
dI_i(t) &= \delta E_i(t-1),\ i = 1, ..., G, t = 1, ..., T \\
dR_i(t) &= \gamma I_i(t-1),\ i = 1, ..., G, t = 1, ..., T \\
dD_i(t) &= \mu_i I_i(t-1),\ i = 1, ..., G, t = 1, ..., T
\end{aligned}
\tag{3}
$$

$$
N_g = S_i(t) + E_i(t) + I_i(t) + R_i(t) + D_i(t),\ g = 1, ..., G, t = 1, ..., T
$$

$$
N = S(t) + E(t) + I(t) + R(t) + D(t),\ t = 1, ..., T
$$

$$
E(t) = \sum_{i=1}^{G} E_i(t),\ I(t) = \sum_{i=1}^{G} I_i(t),\ R(t) = \sum_{i=1}^{G} R_i(t),\ D(t) = \sum_{i=1}^{G} D_i(t),\ t = 1, ..., T
$$

Again, to simulate the course of the epidemic, assuming no NPIs were adopted to mitigate the spread of the infection and flatten the incidence and prevalence curves we assume

$$
dE_i(t) = \psi(t) S_i(t-1) \sum_{j=1}^{G} M'_{ij} \frac{I_j(t-1)}{N_j},\ i = 1, ..., G, t = 1, ..., T \tag{4}
$$

where M'_{ij}, is the time-invariant average daily number of contacts between each pair of age-groups as specified in (6).

This set of equations, jointly with the initial conditions, define the age-structured SEIRD model used in this work.

2.2.3 Contact-mobility matrix

The daily **time-varying contact-mobility matrix**, $\mathbf{M}(t)$ result from scaling the contact matrix of Section 2.1.2 by a mobility index, I(t), as follows:

$$
\mathbf{M}(t) = \mathbf{C} \cdot \mathrm{Idx}(t), \tag{5}
$$

The purpose of Idx(t) is to measure the relative change in baseline contacts due to the implementation of several NPIs, incorporating in the baseline contact matrix $\mathbf{C}$ the adjustments

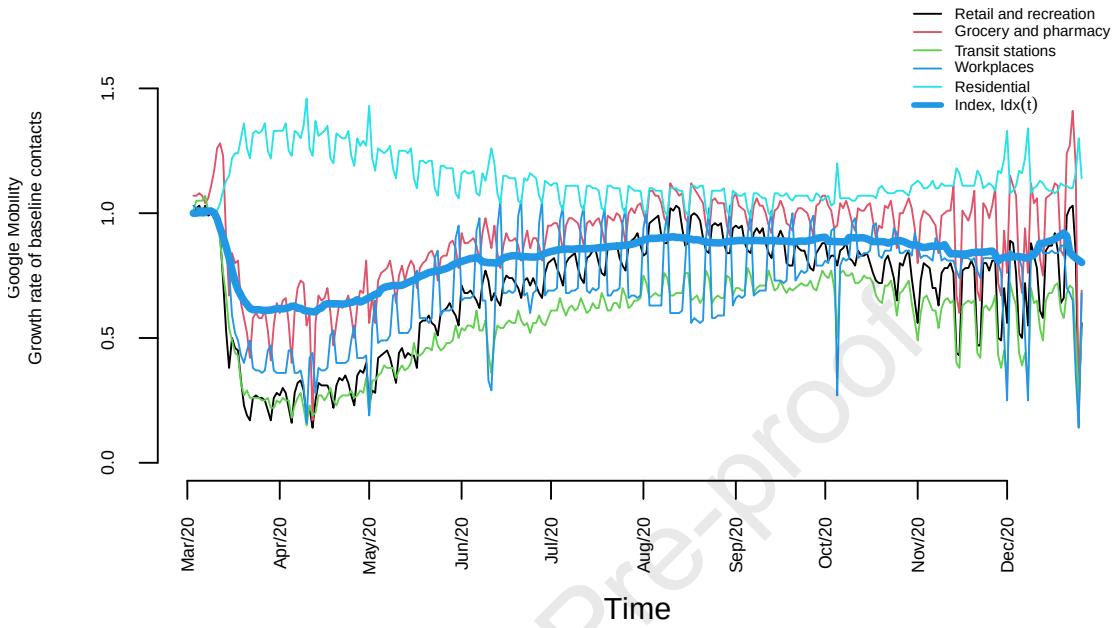

Figure 5: Google mobility. Mobility reported by Google by category and Mobility index used to obtain time-varying contact-mobility matrix.

induced by the NPIs whose role is to limit the contacts between individuals.

The time-varying age-group contact-mobility matrix entries, $M_{ij}(t)$ are conditionally independent random variables as described in Section 2.2.4.

It is generally accepted that flattening the infection incidence curve has been successfully achieved in most European states (e.g. Banholzer et al. (2021), Snoeijer et al. (2021), Suryanarayanan et al. (2021)). However, we do not know what would have happened if the NPIs had not been adopted and, in many cases, enforced by law. Therefore, we decided to perform a simulation where one assumes the contact matrix remains constant, that is,

$$\mathbf{M}' = \mathbf{C}. \tag{6}$$

Here, it is assumed the daily contact rate among people prior to pandemic holds for the whole analysis period, leading to the simulation of what would have been the infection course if the number of contacts among people would mimic the population mixing prior to the pandemic, given the probability of infection caused by a single contact.

The Google Mobility Reports (GMR) data (https://www.google.com/covid19/mobility/),

were used to derive the mobility indexes, $\mathrm{Idx}(t)$. GMR provides daily data on several categories of places are changing in each geographic region. The used categories are: *Retail & recreation*, *Grocery & pharmacy*, *Transit stations*, *Workplaces* and *Residential*. The category *Parks* was not accounted for as the authors consider it has no influence on infections. These five categories originated other five indexes expressed in percentage change of the baseline (prior pandemic) contacts (that is, indexes are greater than 1, if contacts grow; 1, if contacts remain constant; and less than 1, if contacts decrease; see Figure 5). When the lockdown policy was implemented, mobility in workplaces and other locations decreased sharply and increased smoothly again after the measures had been ease. On the contrary, mobility in residential areas shows the opposite course.

These five indexes were collected in the $T \times 5$ matrix of mobility, $\mathbf{W}$. A singular value decomposition of the matrix $\mathbf{W}$, which is admitted to be full-rank, was performed to obtain a single summary index as follows:

$$\mathbf{W} = \mathbf{PEQ}', \tag{7}$$

where $\mathbf{P}$ is a $T \times 5$ matrix, $\mathbf{E}$ is a 5×5 diagonal matrix containing the singular values (square root of eigenvalues) of $\mathbf{W}'\mathbf{W}$ and $\mathbf{Q}'$ is a $5 \times T$ matrix of eigenvectors of $\mathbf{W}'W$. The resulting principals components scores are contained in the columns of the $T \times 5$ matrix $\mathbf{Z}$:

$$\mathbf{Z} = \mathbf{PE} = \mathbf{WQ}. \tag{8}$$

The first principal component (corresponding of first column of the scores matrix $\mathbf{Z}$) accounts for 96.6% of the total variation of the data. Therefore, we used the temporal relative change of these scores as our summary mobility index, $\mathrm{Idx}(t)$, which are represented in Figure 5.

The total number of contacts in Portugal between March, 3^{rd} and December, 26^{th} 2020 (a total of 299 days), the whole period under analysis) can be estimated by:

$$\sum_{t=1}^{T} \sum_{i=1}^{8} \sum_{j \geq i}^{8} M_{ij}(t) N_i.$$

Assuming the situation prior to pandemic had not changed as a result of the set of taken NPIs, the total number of contacts in Portugal in the same period can be estimated by:

$$300 \times \sum_{i=1}^{8} \sum_{j \geq i}^{8} C_{ij} N_i.$$

Therefore, as a result of the changes in mixing and social contacts among citizens, the expected number of contacts decreased from 201015.5 millions to 164418.2 millions. This decay (18.2%) in the number of contacts in the middle of March 2020 was responsible for avoiding millions of infections and thousands of deaths. The results of a simulation comparing these two extreme situations is reported in Section 3.

2.2.4 Bayesian hierarchical model

Using the discrete-time approximation to the stochastic continuous-time SEIRD model (3) defined above we set up a Bayesian hierarchical model where the incidence variables are assumed stochastic (the time unit h is one day).

Bayesian hierarchical models attempt to decompose the observed data into a series of conditional models, all linked together formally through basic probability relationships. In essence the strategy is based on the formulation of three primary statistical models or stages:

- Stage 1: Data model: $[\text{data}|\text{Process}, \boldsymbol{\nu}_1]$,
- Stage 2: Process model: $[\text{Process}|\boldsymbol{\nu}_2]$,
- Stage 3: Prior distributions on parameters: $[\boldsymbol{\nu}_1, \boldsymbol{\nu}_2]$,

where the square brackets notation denotes probability distribution and $\boldsymbol{\nu}_1$ and $\boldsymbol{\nu}_2$ generically represent parameters introduced in the modelling.

The following paragraphs follow this framework describing the (1) likelihood and associated distributional assumptions, (2) the process parameters' link functions and (3) the prior distributions of the model parameters. The section closes with modelling considerations and decisions that have turned model estimation possible.

Table 1 summarises the notation used in the Bayesian hierarchical model likelihood and distributional assumptions below.

2.2.4.1 Likelihood and distributional assumptions Given the three processes defined in the previous section, the likelihood is given as follows:

$$\begin{aligned} \mathcal{L} &= p(\mathbf{dE}, \mathbf{dI}, \mathbf{dR}, \mathbf{dD}, \mathbf{M}|\boldsymbol{\mathcal{M}}, \boldsymbol{\nu}) \\ &= p(\mathbf{dE}|\mathbf{dI}, \mathbf{dR}, \mathbf{dD}, \mathbf{M}, \boldsymbol{\mathcal{M}}, \boldsymbol{\nu}) \\ &\quad \times p(\mathbf{dI}|\mathbf{dR}, \mathbf{dD}, \mathbf{M}, \boldsymbol{\mathcal{M}}, \boldsymbol{\nu}) \\ &\quad \times p(\mathbf{dR}|\mathbf{dD}, \mathbf{M}, \boldsymbol{\mathcal{M}}, \boldsymbol{\nu}) \\ &\quad \times p(\mathbf{dD}|\mathbf{M}, \boldsymbol{\mathcal{M}}, \boldsymbol{\nu}) \\ &\quad \times p(\mathbf{M}|\boldsymbol{\mathcal{M}}, \boldsymbol{\nu}) \end{aligned} \tag{9}$$

where $p(\mathbf{u}, \mathbf{v})$ represents the joint probability density of random vectors $\mathbf{u}$, $\mathbf{v}$ and $p(\mathbf{u}|\mathbf{v})$ represent the conditional density of $\mathbf{u}$, given the vector $\mathbf{v}$, $\boldsymbol{\mathcal{M}}$ represents the SEIRD model and the states of its correspondent compartment (as defined in Table 1) and $\boldsymbol{\nu}$ is vector of all model parameters. To formalise the likelihood we need first to make some assumptions, some of them for computational simplicity, others inspired by the data generation process.

The transitions of individuals from one compartment to the next of in the SEIRD model are considered stochastic movements between the corresponding population compartments. In each period, an individual either stays in or moves on to the next compartment. In reliability

Table 1: Bayesian hierarchical likelihood notation. The data on recoveries are not age-grouped stratified. The time series for compartments $\mathbf{S}_i$, $\mathbf{E}_i$, $\mathbf{I}_i$, R, and $\mathbf{D}_i$ are fully determined by applying SEIRD model equations (3) from given initial conditions, $S_i(0)$, $E_i(0)$, $I_i(0)$, $R(0)$ and $D_i(0)$, $i = 1, ..., 8$.

Notation	Description
$dE_i(t)$	Observed counts of susceptible individuals who become infected in age-group i, $i = 1, 2, ..., 8$, at time t, $t = 1, ..., T$
$dI_i(t)$	Observed counts of infected individuals who become infectious in age-group i, $i = 1, 2, ..., 8$, at time t, $t = 1, ..., T$
$dR(t)$	Observed counts of infectious individuals who recover, at time t, $t = 1, ..., T$
$dD_i(t)$	Observed counts of infectious individuals who perish in age-group i, $i = 1, 2, ..., 8$, at time t, $t = 1, ..., T$
$\mathbf{dE}$	$\{\mathbf{dE}_i, i = 1, ..., 8\}$, Vector of observed counts of susceptible individuals who become infected
$\mathbf{dI}$	$\{\mathbf{dI}_i, i = 1, ..., 8\}$, Vector of observed counts of infected individuals who become infectious
$\mathbf{dR}$	$\{dR(t), t = 1, ..., T\}$, Vector of observed counts of infectious individuals who recover
$\mathbf{dD}$	$\{\mathbf{dD}_i, i = 1, ..., 8\}$, Vector of observed counts of infectious individuals who perish
$S_i(t)$	Observed state of susceptible compartment, in age-group i, $i = 1, ..., 8$, at time t, $t = 1, ..., T$
$E_i(t)$	Observed state of exposed compartment, in age-group i, $i = 1, ..., 8$ at time t, $t = 1, ..., T$
$I_i(t)$	Observed state of infectious compartment, in age-group i, $i = 1, ..., 8$ at time t, $t = 1, ..., T$
$I(t)$	$\sum_{i=1}^{8} I_i(t)$, Observed state of infectious compartment, at time t, $t = 1, ..., T$
$\boldsymbol{\mathcal{M}}$	$\{\mathbf{S}, \mathbf{E}, \mathbf{I}, \mathbf{R}, \mathbf{D}\}$, states of the SEIRD model compartments, where $\mathbf{R} = \{R(t), t = 1, ...T\}$, $\mathbf{S} = \{S_i(t), i = 1, ..., 8;\ t = 1, ...T\}$, and $\mathbf{E}$, $\mathbf{I}$, and $\mathbf{D}$ are defined similarly
$\boldsymbol{\mathcal{M}}(t)$	$\{\mathbf{S}(t), \mathbf{E}(t), \mathbf{I}(t), R(t), \mathbf{D}(t)\}$, Vector of states of the SEIRD model compartments at time t, $t = 1, ..., T$
$M_{ij}(t)$	Average number of contacts observed daily between people of age-group i and age-group j, $i, j = 1, ..., 8$ at time t, $t = 1, ..., T$
$\mathbf{M}_i(t)$	Vector of average number of contacts observed daily between people of age-group i, $i = 1, ..., 8$ at time t, $t = 1, ..., T$
$\mathbf{M}$	$\{\mathbf{M}(t), t = 1, ..., T\}$, Vector of contact-mobility matrices
N_i	Size of population in age-group i, $i = 1, ..., 8$
N	$\sum_{i=1}^{8} N_i(t)$, Size of population
$\mathbf{X}$	Matrix of covariates (dummies) concerning NPIs C1, C2, C3, C4, C5, C6, C7, and C8
$\mathbf{H}$	Matrix of covariates (dummies) concerning NPIs H6, $T \times 3$, where the first column is filled with 1's
$\boldsymbol{\nu}$	Vector of model parameters

analysis, life-time is usually considered to follow an exponential distribution. By analogy, here the time length an individual spends in a compartment is exponentially distributed with some compartment-specific rate $\lambda(t)$. Therefore, the probability of extending the stay by a further period of length h is $\exp(-\lambda(t)h)$ and the probability of leaving is therefore $1-\exp(-\lambda(t)h)$. The summation over the individual Bernoulli trials assuming they are independent and identical for all compartment members, would result in binomial distributions (Diekmann, Heesterbeek, and Metz (1990)). Due to the scale we are working with, we found it useful to take advantage of the approximation of the binomial to the Poisson distribution.

Assumption 1

Given (3), we assume that $\mathbf{dE}$ conditional on $\boldsymbol{\mathcal{M}}(t-1)$, $\mathbf{M}_i(t)$ and $\boldsymbol{\nu}$ is independent in time and among age-groups:

$$\begin{aligned} p(\mathbf{dE}|\mathbf{dI},\mathbf{dR},\mathbf{dD},\mathbf{M},\boldsymbol{\mathcal{M}},\boldsymbol{\nu}) &= p(\mathbf{dE}|\boldsymbol{\mathcal{M}}(t-1),\mathbf{M}_i(t),\boldsymbol{\nu}) \\ &= \prod_{i=1}^{8}\prod_{t=1}^{T} p(dE_i(t)|S_i(t-1),\mathbf{I}(t-1),\mathbf{M}_i(t),\boldsymbol{\nu}). \end{aligned} \tag{10}$$

Assumption 2

Given (3), we assume that $\mathbf{dI}$ conditional on $\boldsymbol{\mathcal{M}}(t-1)$ and $\boldsymbol{\nu}$ is independent in time and among age-groups:

$$\begin{aligned} lllp(\mathbf{dI}|\mathbf{dR},\mathbf{dD},\mathbf{M},\boldsymbol{\mathcal{M}},\boldsymbol{\nu}) &= p(\mathbf{dI}|\boldsymbol{\mathcal{M}}(t-1),\boldsymbol{\nu}) \\ &= \prod_{i=1}^{8}\prod_{t=1}^{T} p(dI_i(t)|E_i(t-1),\boldsymbol{\nu}). \end{aligned} \tag{11}$$

Assumption 3

Given (3), we assume that $\mathbf{dR}$ conditional on $\boldsymbol{\mathcal{M}}(t-1)$ and $\boldsymbol{\nu}$ is independent in time:

$$\begin{aligned} p(\mathbf{dR}|\mathbf{dD},\mathbf{M},\boldsymbol{\mathcal{M}},\boldsymbol{\nu}) &= p(\mathbf{dR}|\mathcal{M}(t-1),\boldsymbol{\nu}) \\ &= \prod_{t=1}^{T} p(dR(t)|I(t-1),\boldsymbol{\nu}). \end{aligned} \tag{12}$$

Assumption 4:

Given (3), we assume that $\mathbf{dD}$ conditional on $\boldsymbol{\mathcal{M}}(t-1)$ and $\boldsymbol{\nu}$ is independent in time and

among age-groups:

$$\begin{aligned} p(\mathbf{dD}|\mathbf{M}, \boldsymbol{\mathcal{M}}, \boldsymbol{\nu}) &= p(\mathbf{dD}|\boldsymbol{\mathcal{M}}(t-1), \boldsymbol{\nu}) \\ &= \prod_{i=1}^{8}\prod_{t=1}^{T} p(dD_i(t)|I_i(t-1), \boldsymbol{\nu}). \end{aligned} \tag{13}$$

Assumption 5

The incidences $dE_i(t)$, $dI_i(t)$, $dR_i(t)$, and $dD_i(t)$ are considered conditionally independent Poisson random variables, that is:

$$\begin{aligned} p(dE_i(t)|S_i(t-1), \mathbf{M}_i(t), \mathbf{I}(t-1), \boldsymbol{\nu}) &\sim \text{Pois}(S_i(t-1) \times \pi_{dE_i}(t)),\ i = 1, ..., 8, t = 1, ..., T \\ p(dI_i(t)|E_i(t-1), \boldsymbol{\nu}) &\sim \text{Pois}(E_i(t-1) \times \pi_{dI_i}(t)),\ i = 1, ..., 8, t = 1, ..., T \\ p(dR(t)|I(t-1), \boldsymbol{\nu}) &\sim \text{Pois}(I(t-1) \times \pi_{dR}),\ i = 1, ..., 8, t = 1, ..., T \\ p(dD_i(t)|I_i(t-1), \boldsymbol{\nu}) &\sim \text{Pois}(I_i(t-1) \times \pi_{dD_i}(t)),\ i = 1, ..., 8, t = 1, ..., T, \end{aligned} \tag{14}$$

where transition probabilities are given by:

$$\begin{aligned} \pi_{dE_i}(t) &= 1 - \exp\left(-\psi(t)\sum_{j=1}^{G} M_{ij}(t)\frac{I_j(t-1)}{N_j},\ i, j = 1, ..., 8, t = 1, ..., T\right), \\ \pi_{dI_i} &= 1 - \exp\left(-\delta\right),\ i = 1, ..., 8, t = 1, ..., T \\ \pi_{dR} &= 1 - \exp\left(-\gamma\right),\ i = 1, ..., 8, t = 1, ..., T \\ \pi_{dD_i}(t) &= 1 - \exp\left(-\mu_i(t)\right)\ i = 1, ..., 8, t = 1, ..., T. \end{aligned} \tag{15}$$

The model further assumes the population size is $N = \sum_{i=1}^{8} N_i$, remains constant, and individuals mix homogeneously.

Assumption 6

The time-varying age-group contact-mobility matrix entries, $M_{ij}(t)$, are considered stochastic, conditionally independent, given a set of covariates that impact, directly or indirectly, in the contacts as depicted by the stringency of the NPIs of Table 2. The model matrix $\mathbf{X}$ is a matrix containing dummy variables for each level of stringency as described in Table 2. Due to collinearity issues, some of the stringency levels on Table 2 result from aggregation of the raw ones as explained below.

The three levels of stringency of C1(t), $t = 1, ..., T$, were collapsed into two levels as we think the distinction between *recommendation* and *requirement* is useless given that the public education system in Portugal (representing 98% of the sector) complied quickly with all the interventions and even anticipated them. The four levels of stringency of C4(t), $t = 1, ..., T$,

were collapsed in a single one as we think the distinction based on the size of the gatherings is useless for our purposes. Due to Spearman's perfect correlation between C3(t) and C4(t) and highly collinearity of these and C8(t) with C1(t), we removed variables C3(t), C4(t), and C8(t) from the analysis, letting C1(t) as being their proxy. This prevents the Markov chain chain simulation process from mixing poorly being unable to distinguish the effects of those variables on the contact-mobility levels. Therefore, the model matrix is defined as: $\mathbf{X} = (\mathbf{C1}_1, \mathbf{C2}_1, \mathbf{C2}_2, \mathbf{C5}_1, \mathbf{C6}_1, \mathbf{C6}_2, \mathbf{C7}_1)$, where $\mathbf{C1}_1 = \{\mathrm{C1}_1(t), t = 1, ..., T\}$ is the vector of T observations of the dummy variable representing the stringency level 1 of C1(t) and the remaining variables are defined in a similar manner. Moreover, the time-varying age-group contact-mobility matrix entries are considered conditionally independent and follow a gamma model as follows:

$$p(M_{ij}(t)|\mathbf{X}) \sim \mathrm{Ga}\left(\theta_i, \frac{\theta_i}{\xi_{ij}(t)}\right), \; i, j = 1, ..., 8, t = 1, ..., T \tag{16}$$

where θ_i is the shape parameter and $\dfrac{\theta^g}{\xi_{ig}(t)}$ is the rate parameter, implying $\mathrm{E}(M_{ij}(t)|\mathbf{X}) = \xi_{ij}(t)$.

The above assumptions simplify the likelihood as follows:

$$\begin{aligned}
\mathcal{L} &= p(\mathbf{dE}, \mathbf{dI}, \mathbf{dR}, \mathbf{dD}, \mathbf{M}) \\
&= p(\mathbf{dE}|\mathbf{dI}, \mathbf{dR}, \mathbf{dD}, \mathbf{M}) p(\mathbf{dI}|\mathbf{dR}, \mathbf{dD}, \mathbf{M}) p(\mathbf{dR}|\mathbf{dD}, \mathbf{M}) p(\mathbf{dD}|\mathbf{M}) p(\mathbf{M}) \\
&= \prod_{t=1}^{T} p\left(dR(t)|I(t-1)\right) \prod_{i=1}^{8} p\left(dE_i(t)|S_i(t-1), \mathbf{I}(t-1), \mathbf{M}_i(t)\right) \\
&\quad \times p\left(dI_i(t)|E_i(t-1)\right) p\left(dD_i(t)|I_i(t-1)\right) \prod_{j=1}^{8} p\left(M_{ij}(t)\right)
\end{aligned} \tag{17}$$

2.2.4.2 Link functions In order to account for the effects of some NPIs such as lockdown and social distancing, we assume that the transmission rate is affected by: (1) the time-varying age-group contact-mobility matrix $\mathbf{M}(t)$ or the constant age-group specific contact-mobility matrix $\mathbf{M}'$ (obtained as explained in Section 2.2.3) and (2) the probability of virus transmission $\psi(t)$, which is assumed to be a step function where the intervention moments correspond to the entry in force of an important self-protection measure not accounted for by mobility indexes, that is, the use of facial coverings. It is modelleded through two dummy variables $\mathrm{H6}_1(t)$ and $\mathrm{H6}_2(t)$:

$$\mathrm{H6}_1(t) = \begin{cases} 1, & \mathrm{H6}(t) = 1 \\ 0, & \text{otherwise} \end{cases}, \; t = 1, ..., T, \tag{18}$$

$$\mathrm{H6}_2(t) = \begin{cases} 1, & \mathrm{H6}(t) = 2 \\ 0, & \text{otherwise} \end{cases}, \; t = 1, ..., T, \tag{19}$$

Table 2: Non-pharmaceutical interventions and corresponding levels considered in this work

Name	Coding
(C1) School closing	0 - no measures 1 - Recommend closing or all schools open with alterations resulting in significant differences compared to non-Covid-19 operations **or** require closing (only some levels or categories, e.g. just high schools, or just public schools) **or** require closing all levels ($C1_1$)
(C2) Workplace closing	0 - no measures 1 - require closing (or work from home) for some sectors or categories of workers ($C2_1$) 2 - require closing (or work from home) for all-but-essential workplaces (e.g. grocery stores, doctors) ($C2_2$)
(C5) Close public transport	0 - no measures 1 - recommend closing (or significantly reducing volume/route/means of transport available) ($C5_1$)
(C6) Stay at home requirements	0 - no measures 1 - recommend not leaving house ($C6_1$) 2 - require not leaving house with exceptions for daily exercise, grocery shopping, and 'essential' trips ($C6_2$)
(C7) Restrictions on internal movement	0 - no measures 1 - recommend not to travel between regions/cities or internal movement restrictions in place ($C7_1$)
(H6) Facial coverings	0 - No policy 1 - Required in some specified shared/public spaces outside the home with other people present or in some situations when social distancing is not possible ($H6_1$) 2 - Required in all shared/public spaces outside the home with other people present or all situations when social distancing is not possible ($H6_2$)

which correspond to the periods when facial coverings were *required in some specified shared/public spaces outside the home with other people present, or some situations when social distancing was not possible* (cf. Table 2) and when they were *required in all shared/public spaces outside the home with other people present or all situations when social distancing was not possible* (cf. Table 2).

This implies $\psi(t)$ to be formulated as:

$$\text{logit}(\psi(t)) = \mathbf{H}'(t)\boldsymbol{\eta} = \eta_0 + \eta_1 \text{H6}_1(t) + \eta_2 \text{H6}_2(t) = \begin{cases} \eta_0 & t < \tau_1 \\ \eta_0 + \eta_1, & \tau_1 \leq t < \tau_2 \\ \eta_0 + \eta_2, & t \geq \tau_2 \end{cases}, \; t = 1, ..., T, \tag{20}$$

where logit($\bullet$) is the $\log(p/(1-p))$ transformation, $\boldsymbol{\eta'} = (\eta_0, \eta_1, \eta_2)$, where η_0 is the baseline probability that a contact provokes the transmission of the disease, η_1 and η_2 are the (expected) change in this probability due to the introduction of two different stringency levels of wearing a facial covering and $\mathbf{h}'(t)$ is the t^{th} row of the $T \times 3$ matrix $\mathbf{H}$, composed of a column of 1's and the two T-length column vectors representing the dummy variables describing the stringency of wearing facial coverings (H6(t)), $\mathbf{H} = (\mathbf{1}, \text{H}\mathbf{6}_1, \text{H}\mathbf{6}_2)$. This formulation allows for assessing the effect of the introduction of facial coverings on the risk of getting infected.

The link function for $\xi_{ij}(t)$ in (16) is defined by:

$$\log\left(\xi_{ij}(t)\right) = \lambda_{ij}^0 + \mathbf{x}'(t)\boldsymbol{\lambda}, \; i, j = 1, ..., 8; \; t = 1, \ldots, T, \tag{21}$$

where λ_{ij}^0 models the expected log-level value of the baseline contact-mobility matrix $M_{ij}(1)$ (that is, C_{ij}), and $\boldsymbol{\lambda} = (\lambda^{\text{C1}_1}, \lambda^{\text{C2}_1}, \lambda^{\text{C2}_2}, \lambda^{\text{C5}_1}, \lambda^{\text{C6}_1}, \lambda^{\text{C6}_2}, \lambda^{\text{C7}_1})$ are the regression coefficients multiplying $\mathbf{x}'(t)$, $t = 1, ..., T$, the rows of $\mathbf{X}$ (as defined before).

The expected value of the gamma distribution above is defined to assess NPI effects on the average number of daily contacts responsible for infection spreading. The mean of the posterior distribution of $\exp(\lambda_{ij}^0)$, $t = 1$, is expected to fit the entries of the contact matrix $\mathbf{C} = [C]_{i,j=1}^8$, and the posterior mean of $\exp(\mathbf{X}'\boldsymbol{\lambda})$ is meant to fit the mobility index Idx(t), $t = 1, ..., T$ defined in Section 2.2.3.

A comment on the previous model matrix is necessary. The authors think the facial coverings interventions (H6) may be better accounted for in the model of probability of virus transmission, ψ, as it might might be seen as an reduction on the baseline probability of infection. As a matter of fact, several other authors have used this framework to assess the potential effect of using masks (e.g., Eikenberry et al. (2020) and Leech et al. (2022)).

Evoking the aforementioned reasons (cf. Section 2.2.2), the parameters $\mu_i(t)$, $i = 1, ..., 8$, which govern the passage from the compartment I to the compartment D, are considered age-group dependent. For the first four age groups, [0,9], [10,19], [20,29] and [30,39] deaths

are rare; therefore the fatality rate is considered time-invariant:

$$\mu_i(t) = \mu_i^0,\ i = 1, 2, 3, 4,\ t = 1, ..., T, \tag{22}$$

For the last four age-groups, [40,49], [50,59], [60,69] and 70+ the parameters $\mu_i(t)$ are considered time-dependent following an exponentially decreasing trend, with an increasing rate constant across the four age-groups:

$$\mu_i(t) = \mu_i^0 \exp(-\rho_\mu t),\ i = 5, 6, 7, 8,\ t = 1, ..., T, \tag{23}$$

where the parameter μ_i^0, $i = 5, 6, 7, 8$, represents the initial value of the fatality rate.

As discussed about the SEIRD model represented in Figure 4, the fatality rates, $\mu_{(.)}(t)$ in (22) and (23) represent the product of two distinct quantities: (1) the probability of moving from compartment I to compartment D and (2) the inverse of the period an infected person takes to perish. It is measured in $days^{-1}$. The mortality rate is supposed to decrease over time at a rate of ρ_μ (expressed in days).

2.2.4.3 Prior distributions The following independent prior distributions are assigned to each of the previous parameters:

$$\begin{array}{lcl}
\boldsymbol{\eta} & \sim & \mathrm{N}_3(\mathbf{0}, \mathbf{P}_\eta), \\
\lambda_{ij}^0 & \sim & \mathrm{N}(0, 0.0001),\ i, j = 1, ..., 8, \\
\boldsymbol{\lambda} & \sim & \mathrm{N}_7(\mathbf{0}, \mathbf{P}_\lambda), \\
\theta_i & \sim & \mathrm{Ga}(0.0001, 0.0001),\ i = 1, ...8 \\
\mu_i & \sim & \mathrm{Ga}(0.0001, 0.0001),\ i = 1, ...8, \\
\rho_\mu & \sim & \mathrm{Ga}(0.0001, 0.0001).
\end{array} \tag{24}$$

where $\mathrm{Ga}(a, b)$ refers to a gamma distribution with shape a and rate b, mean a/b, and variance a/b^2, $\mathrm{N}(0, 0.0001)$ to a normal distribution with a mean of zero and a precision of 0.0001, and $\mathrm{N}_{(\bullet)}(\mathbf{0}, \mathbf{P}_{(\bullet)})$ to a $(\bullet)$-variate multivariate normal distribution with a mean vector of zeros and precision matrix $\mathbf{P}_{(\bullet)}$. The precision matrix $\mathbf{P}_\bullet$ follows a Wishart distribution with a diagonal scale matrix with diagonal elements equal to 1000 and $\dim(P_{(\bullet)}) + 2$ degrees of freedom to ensure a non-informative hyperprior.

Given the hierarchical representation presented above and using the same notation as in (17), one can evaluate the posterior distribution of all of the processes and parameters, given the

observed data:

$$
\begin{aligned}
&\Pi(\boldsymbol{\nu}|\mathbf{dE},\mathbf{dI},\mathbf{dR},\mathbf{dD},\mathbf{M},\mathbf{X},\mathbf{H}) \propto p(\mathbf{dE},\mathbf{dI},\mathbf{dR},\mathbf{dD},\mathbf{M}|\boldsymbol{\nu},\mathbf{X},\mathbf{H})p(\boldsymbol{\nu}) \\
&= p(\mathbf{dE},\mathbf{dI},\mathbf{dR},\mathbf{dD},\mathbf{M}|\boldsymbol{\nu},\mathbf{X},\mathbf{H})p(\boldsymbol{\eta}) \left[\prod_{i=1}^{8}\prod_{j=1}^{8} p(\lambda_{ij}^{0})\right] p(\boldsymbol{\lambda})p(\boldsymbol{\theta})p(\boldsymbol{\mu})p(\rho_{\mu}) \\
&= \prod_{t=1}^{T} p\left(dR(t)|I(t-1)\right) \prod_{i=1}^{8} p\left(dE_i(t)|S_i(t-1),\mathbf{I}(t-1),\mathbf{M}_i(t)\right) \\
&\times p\left(dI_i(t)|E_i(t-1)\right) p\left(dD_i(t)|I_i(t-1)\right) \prod_{j=1}^{8} p\left(M_{ij}(t)\right) \\
&\times p(\boldsymbol{\eta}) \left[\prod_{i=1}^{8}\prod_{j=1}^{8} p(\lambda_{ij}^{0})\right] p(\boldsymbol{\lambda})p(\boldsymbol{\theta})p(\boldsymbol{\mu})p(\rho_{\mu})
\end{aligned}
\tag{25}
$$

2.2.4.4 Other considerations The epidemic model specified in (3), (4), (14) and (15), the fatality rate models (22) and (23) with the transmission probability model (20), and the time-varying age-group contact-mobility matrix model (16) and (21) has parameter vector $\boldsymbol{\nu} = (\boldsymbol{\eta}, \lambda_{1,1}^{0}, \lambda_{1,2}^{0}, ..., \lambda_{8,8}^{0}, \boldsymbol{\lambda}, \boldsymbol{\theta}, \boldsymbol{\mu}, \rho_{\mu})$, which we would like to estimate from the knowledge of the initial conditions $S_i(0)$, $E_i(0)$, $I_i(0)$, $R_i(0) = 0$, and $D_i(0) = 0$, $i = 1, ..., 8$, the population sizes, N_i, $i, 1, ..., 8$, and the data of $\{\mathbf{dE}, \mathbf{dI}, \mathbf{dR}, \mathbf{dD}, \mathbf{M}, \mathbf{X}, \mathbf{H}\}$.

The initial conditions $I_i(0)$, $i = 1, ..., 8$ are unknown. Indeed, the number of confirmed cases in the very beginning of the epidemic is far from the true prevalence of COVID-19 infections. However, for simplicity, one assumes it to be known and equals the number of confirmed infected cases on March 3^{rd}, 2020, in each age-group. To determine the initial conditions $S_i(0)$, $E_i(0)$, $i = 1, ..., 8$, one needs to know at least one of them. One decided to estimate the initial condition $E_i(0)$, $i = 1, ..., 8$ from the series of exposed, $dE_i(t)$, whose paths were based on the time between exposure and infectiousness, that is, 5.1 days, on average (Mendes and Coelho (2021)). A gamma distribution with a μ_X/σ_X parameter of 5.1/4.5, corresponding to a mean and median incubation period of 5.1 and 4.2 days was used to backcast the values of $dI_i(t)$ to the previous compartment and provide the initial values $E_i(0)$, $i = 1, ..., 8$. The initial conditions $S_i(0)$, $i = 1, ..., 8$ were then obtained by difference to the total population of the respective age-group, N_i, $i = 1, ..., 8$. This procedure was only used to estimate the initial conditions $S_i(0)$ and $E_i(0)$. Indeed, the observed processes $dE_i(t)$, $i = 1, ..., 8$, $t = 1, ...T$ are not observed and thus considered missing, requiring numeric integration over the support of the probability distribution of $dE_i(t)$ in (25).

One cannot evaluate the posterior distribution (25) analytically and must resort to numeric simulation methods. We use the special case of MCMC known as Gibbs sampling (Gilks, Richardson, and Spiegelhalter (1996)) and implemented the algorithm using the `R` package `JAGS` (all code used in this paper can be obtained from the authors upon request).

Additionally to the estimation of model parameters $\boldsymbol{\nu}$, we decided to perform four additional simulations to assess the effect of the absence of *all/some* NPIs on infections. The first

considers the case where no NPIs are considered, except facial coverings (denoted in the Section 3 as *Facial coverings(+), other NPIs(-)*). The second accounts for all NPIs effects are considered but facial coverings (denoted in the Section 3 as *Facial coverings(-), other NPIs(+)*). The third accounts for the case where no NPIs effects are considered (denoted in the Section 3 as *Facial coverings(-), other NPIs(-)*). This simulation in based on a constant transmission probability $\psi(t) = \eta_0$ and a constant contact-mobility matrix, that is $\mathbf{M}' = \mathbf{C}$. Finally, the fourth simulation accounts only for the effects of *Facial coverings* and *Workplace closing* (denoted in the Section 3 as *Facial coverings(+), Workplace closing(+)*).

3 Results

After an adaptation phase of 5,000 iterations and a burn-in period of 2,000 iterations by which we consider convergence has been achieved. A sample of size of 300, resulting from running four independent chains with a thin step of 50 iterations (to avoid serial correlation) was used to obtain marginal posterior distributions for all model parameters. For the vast majority of the parameters the Gelman-Rubin statistic (Brooks and Gelman (1998)) achieved values below 1.05 which reinforces the belief convergence was achieved (cf. Table A2 in Appendix).

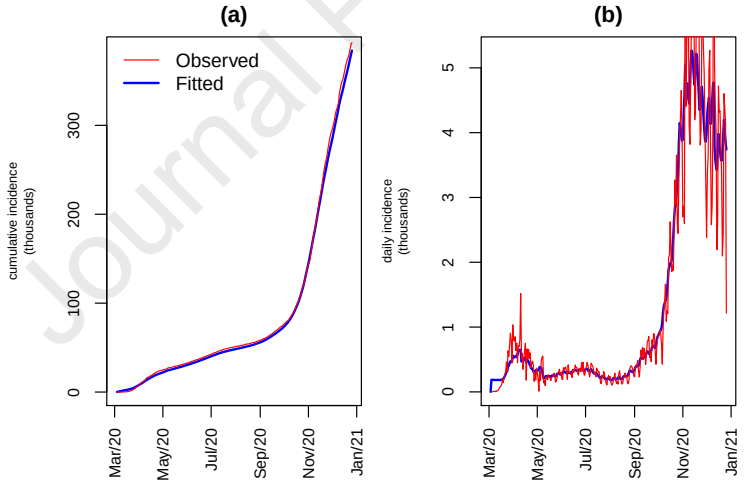

Figure 6: Model fitting results on infections. (a) Observed daily accumulated cases of infection (red) and mean of predictive distribution of $\sum_t dI(t)$, $\sum_t \mathrm{E}[dI(t)]$ (blue). (b) Observed daily confirmed cases of infection (red) and mean of predictive distribution of $dI(t)$, $\mathrm{E}[dI(t)]$ (blue).

Analysing the model's fit against real data is relevant as a tool of external validation. Therefore, the model fit is assessed by plotting the available data against the estimated expected values of the posterior distribution. The model's fit is evident from Figures A1 and A2, in the Appendix, regarding the age-group epidemic data, and Figures 6, 7 and 8 for accumulated and daily number of infected cases, accumulated deaths and recoveries, regarding all ages, for the period corresponding to the used data. Indeed, the observed

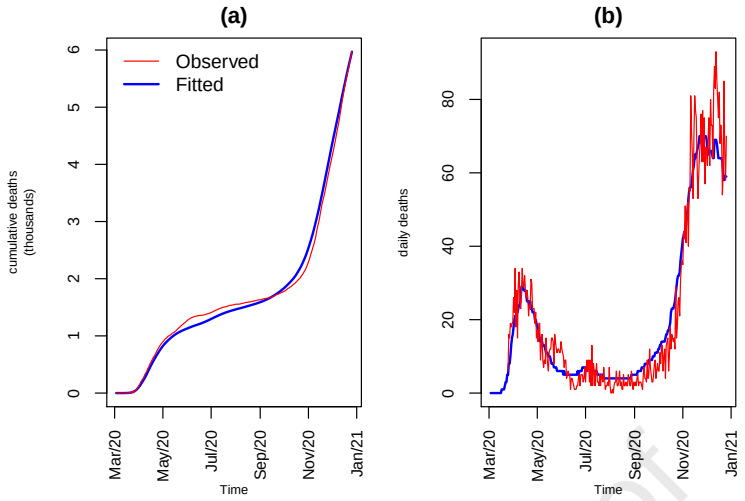

Figure 7: Model fitting results on deaths. (a) Observed daily accumulated deaths (red) and mean of predictive distribution of $\sum_t dD(t)$, $\sum_t \mathrm{E}[dD(t)]$ (blue). (b) Observed daily daily deaths (red) and mean of predictive distribution of $dD(t)$, $\mathrm{E}[dD(t)]$ (blue).

number of accumulated infected cases, $\sum_t dI(t)$, is 391.7 thousands and the fitted value, $\sum_t \mathrm{E}[dI(t)]$, is 384.1 thousands, representing an underestimation of about 1.9%; on the other hand, the observed number of accumulated deaths for the period under analysis, $D(t)$ on 26^th December, 2020, is 5907 and the fitted value, $\sum_t \mathrm{E}[dD(t)]$, is 5911, representing an overestimation of only 0.07%.

The contact-mobility matrix, $\mathbf{M}(t)$, and its baseline source $\mathbf{C}$ and mobility index $\mathrm{Idx}(t)$ (see Section 2.2.3), are targets of the proposed model. Therefore, Figures A3 and A4 summarise model's fitting results regarding the mobility index $\mathrm{Idx}(t)$, and the contact matrix $\mathbf{C}$. Figure A3 shows the mobility index, $\mathrm{Idx}(t)$, $t = 1, ..., T$ and the mean of posterior distribution of $\exp(\mathbf{X}\boldsymbol{\lambda})$ (see equation (21)). It fairly follows the mobility index temporal path.

Finally, Figure A4 shows, side by side, the target matrix $\mathbf{C}$ and the mean of the marginal posterior distribution of $\exp(\lambda^0_{ij})$, $i, j = 1, ..., 8$. Some small differences are noticed but the 5-tone colour pattern is similar in both matrices. Moreover, the root mean square deviation between the entries of $\mathbf{C}$ and their fitted values is equal to 0.06 daily contacts.

These results suggest that jointly considering a time-varying probability of infection, $\psi(t)$, and a time-varying contact-mobility matrix is able to capture the age-group and the overall course of the epidemic. It also confirms something else: mobility data, represented here through the Google Mobility data, mimics the reduction in daily contacts among individuals which inevitably led to mitigating the natural spread of the disease.

Figure 8(a) represents the overall number of recovery people paths (as mentioned previously age-group recovery data are unavailable). As described in Section 2.2.4, we considered the recovery rate, γ, as a fixed parameter. The purpose was to mimic the recovery path using a

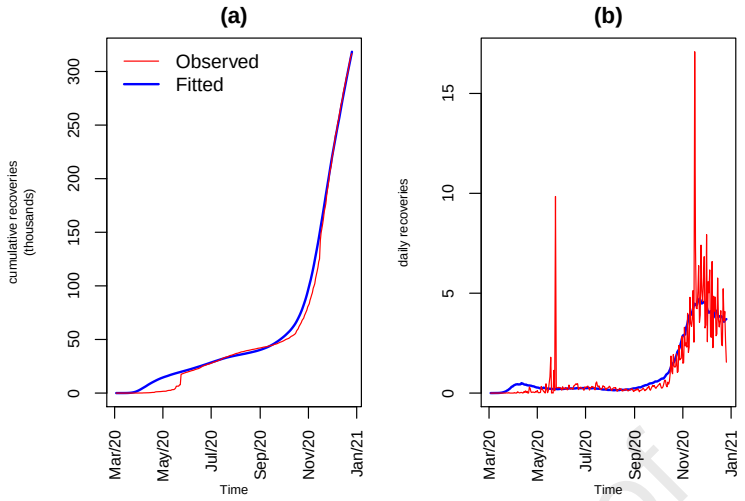

Figure 8: Model fitting results on recoveries. (a) Observed daily accumulated recoveries (red) and mean of predictive distribution of $\sum_t dR(t)$, $\sum_t \mathrm{E}[dR(t)]$ (blue). (b) Observed daily daily recoveries (red) and mean predictive distribution of $dR(t)$, $\mathrm{E}[dR(t)]$ (blue).

generally literature-accepted recovery rate (corresponding to 14 days of infectiousness) and compare it with the non-reliable figures released by national heath authorities. As Figure 8 shows, the estimated path of recoveries shows some departure from the observed one, confirming the expert perception of the delay of releasing figures about infected people off the isolation period followed a conservative criterion. Besides, the spikes in the observed path denote the moments when DGS released data on recoveries accumulated for some weeks.

Table 3 presents the posterior means and posterior standard deviations of model parameters. The results regarding the infection parameters equation (20) are all statistically significant at 5%. The posterior mean of η_1 is -0.513 (se=0.010). Therefore, the risk of a contact provokes the transmission of the disease suffers a reduction of 40.2% $(1 - \exp(\eta_1) \times 100)$, when facial coverings become *required in **some** specified shared/public spaces outside the home with other people present, or **some** situations when social distancing not possible.* Moreover, when the stringency of this NPI increased, that is, when facial covering become *required in **all** shared/public spaces outside the home with other people present or **all** situations when social distancing not possible* the risk fall down even sharply by 59.0%, as the posterior mean of η_2 is -0.892.

The results regarding the age-group fatality rates, μ_i, $i = 1, ..., 8$ are also reported. These parameters are expressed in days $^{-1}$ units. They are not significantly different from zero (at 5% significance level) for the first two age-groups, [0,9] and [10,19] years of age. For the age-groups [20,29] and [30,39] fatality rates are statistically significant but still not different from zero in practical terms. For older ages, the results, being statistically significant, are not practically different from zero. In the period under analysis Portugal undergone a pandemic landscape dominated by the variant *alpha* of SARS-CoV-2 which was not one of deadliest

Table 3: Posterior means, standard deviations and p-values of the estimated Bayesian hierarchical SEIRD model

Parameter	Posterior mean (std)	p-value
η_0	-6.004 (0.009)	0.00
η_1	-0.513 (0.01)	0.00
η_2	-0.892 (0.009)	0.00
μ^1	5×10^{-6} (5×10^{-6})	0.18
μ^2	3×10^{-6} (3×10^{-6})	0.16
μ^3	4×10^{-6} (2×10^{-6})	0.04
μ^4	9×10^{-6} (4×10^{-6})	0.00
μ^5	5.1×10^{-5} (1.2×10^{-5})	0.00
μ^6	1.36×10^{-4} (2.1×10^{-5})	0.00
μ^7	5.49×10^{-4} (4.9×10^{-5})	0.00
μ^8	0.015754 (5.57×10^{-4})	0.00
ρ_μ	0.00289 (1.55×10^{-4})	0.00
θ_1	425.428 (9.461)	0.00
θ_2	426.769 (9.302)	0.00
θ_3	425.855 (11.818)	0.00
θ_4	425.122 (12.647)	0.00
θ_5	425.438 (14.446)	0.00
θ_6	426.489 (17.431)	0.00
θ_7	424.998 (24.956)	0.00
θ_8	25.7 (59.4)	0.33

among all SARS-CoV-2 variants identified so far. Moreover, the fatality rate μ here represents the product of the probability of an infectious individual die (α) by the rate (in days) it takes to perish (μ') (see Section 2.2.1). The estimated value of μ_8, given by the mean of its marginal posterior distribution is $\hat{\mu}_8 = 0.0157538$. If we assume that only a tiny fraction of the infectious individuals go through a serious respiratory condition leading eventually to death, usually reported between 1% and 4% (the value of α), that it would correspond to a average of between 0.5 and 2.5 days to perish after becoming infectious, that is, hosting a sufficient viral load capable of spreading out to other individuals.

Table 4 shows the expected impact (in per cent) of the combination NPI/level considered in this work on the average contact-mobility matrix entries. The values were computed transforming the posterior means of the log link function} (21), $(\exp(\lambda^{(\bullet)}) - 1) \times 100$. The statistical significance of the parameter (at 5% significance level) is indicated in the table by the superscript "^{a}".

The results show that, holding the other NPIs fixed, on average, *closing (or working from home) for some sectors or categories of workers* ($C2_1$, starting on March 12^{th} 2020) had a statistically significant effect on reducing prior pandemic contact-mobility levels by 14.19%. However, when this NPI became more strict (*closing (or working from home) for all-but-essential workplaces (e.g. grocery stores, doctors)* ($C2_2$, starting on March 19^{th} 2020), the

Table 4: Results on the link functions of the contact-mobility matrix gamma model. Statistically significant parameters at 5% level are indicated by superscript "^{a}". Results are indicated in ±% variation on mobility from baseline ($(\exp(\lambda^{(\bullet)}) - 1) \times 100\%$) where "$\bullet$" represents the combination NPI/level.

NPI	Level	%
School closing (C1)	Recommend closing or all schools open with alterations resulting in significant differences compared to non-Covid-19 operations **or** require closing (only some levels or categories, e.g. just high school, or just public schools) **or** require closing all levels ($C1_1$)	-0.59
Workplace closing (C2)	Require closing (or work from home) for some sectors or categories of workers ($C2_1$)	-14.19^a
	Require closing (or work from home) for all-but-essential workplaces (e.g. grocery, stores, doctors) ($C2_2$)	-35.57^a
Close public transport (C5)	Recommend closing (or significantly reduce volume/route/means of transport available) ($C5_1$)	2.16^a
Stay at home requirements (C6)	Recommend not leaving house ($C6_1$)	-8.08^a
	Require not leaving house with exceptions for daily exercise, grocery shopping, and 'essential' trips ($C6_2$)	-1.68^a
Restrictions on internal movement (C7)	Recommend not to travel between regions/cities **or** internal movement restrictions in place ($C7_1$)	-2.45^a

prior pandemic contact-mobility levels dropped, on average by 35.57%.

The result on *recommend not leaving house* ($C6_1$, stating on March 15^{th} 2020) shows it had more impact in reducing the prior pandemic contact-mobility levels (-8.08%), than *requiring not leaving the house with exceptions for daily exercise, grocery shopping, and 'essential' trips* ($C6_2$), which started four days later, on March 19^{th} 2020 (-1.68%). A behaviour of self protection may explain this result, as at the beginning of the pandemic, a generalised feeling of fear spread out in the Portuguese population.

Much debate is going on about the effect of *School closing* ($C1_1$, starting on March 9^{th} 2020). Results presented in Table 4 on school closing do not indicate a high potential for reduction of prior pandemic contact-mobility levels (-0.59%). This NPI mainly aimed at preventing students to infect their families after infectious contacts at school environment and the other way around. Its lack of effect is likely due to its nature that did not have direct effects on the generalised contact-mobility levels.

Table 4 also reports the estimated impact of two other combinations NPI/level. First, The result regarding *recommend closing public transport (or significantly reduce volume/route/means of transport available)* ($C5_1$, starting on March 19^{th} 2020) shows a statistically significant impact on raising the prior pandemic contact-mobility levels (2.16%). This result is not surprising as we know that limitations on the offer of public transportation may, on one hand prevent close contacts among passengers but, on the other hand, may imply the citizens to move around using other transportation means and thus raising the contact-mobility levels as they are measured in this work. Second, the result regarding *recommend not to travel between regions/cities or internal movement restrictions in place* ($C7_1$, starting on March 19^{th} 2020) exhibits a marginal, but still statistically significant, impact on reducing the prior pandemic contact-mobility levels by only 2.45%.

Three other NPIs that were not considered for model estimation *Cancel public events*, (C3), *Restrictions on gatherings* (C4), and *International travel controls* (C8) as explained in Section 2.2.4. In Portugal, these measures were in place for a extended period of time (cf. Figure 2) and were almost coincident (collinear) with *school closing*. Results about their proxy, C1, suggest they had a small or even null impact on changing the prior pandemic contact-mobility levels.

Table 5: Results of simulations on December, 26^{th} 2020, considering the absence of all or some NPIs

Measure	Accumulated infections	Accumulated deaths	Daily maximum infections
Observed	391.7 thous.	5907 thous.	9.2 thous.
Simulation 1 (*Facial coverings(+), other NPIs(-)*)	8.2 mill.	88.5 thous.	107.8 thous.
Simulation 2 (*Facial coverings(-), other NPIs(-)*)	9.7 mill.	147.3 thous.	225.0 thous.
Simulation 3 (*Facial coverings(-), other NPIs(+)*)	9.4 mill.	122.7 thous.	181.8 thous.
Simulation 4 (*Facial coverings(+), Workplace closing(+)*)	7.1 mill.	59.8 thous.	75.7 thous.

The results of the four simulations performed are presented in Table 5 and Figures A5, A6 and A7. The results suggest a very much different situation on December 26^{th}, 2020 regarding the accumulated number of infections, the daily infections and deaths under different NPI scenarios.

In simulation 1 we consider a situation where measures are absent, except for facial coverings (one denotes it as *Facial coverings(+), other NPIs(-)*). This simulation shows the number

of accumulated infections by December 26^{th} would reach 8.2 million, instead of the 391.7 thousand actually verified. Similarly, this simulation shows the accumulated number of deaths would reach 88.5 thousand instead of the 5907 observed indeed. On the other hand, the maximum of daily number of infection cases would reach 107.8 thousands, a much larger number than the recorded daily maximum on December, 9^{th} 2020 (9.2 thousand).

Simulation 2 represents an even more extreme scenario (one denote it as *Facial coverings(-), other NPIs(-)*) . Indeed, in the absence of any NPI, including neither the mandatory use of facial coverings in **some** or **all** places, the number of accumulated infections by December 26^{th} would reach 9.7 million, the accumulated deaths would reach 147.3 thousand, and the maximum of daily infection would reach 225.0 thousand.

Simulation 3 represents an intermediate situation somewhere between simulations 1 and 2 (one denotes it as *Facial coverings(-), other NPIs(+)*). Indeed, in the absence of facial covering, but assuming all other NPIs were taken, the number of accumulated infections by December 26^{th} would reach 9.4 million, the accumulated deaths would reach 122.7 thousand, and the maximum of daily infections would reach 181.8 thousand.

Simulation 3 shows that the joint adoption of a set of NPI whose intended role was to prevent people from closely contacting each other, has a more extensive impact than the universal use of facial coverings. Yet, the use of facial masks together with the additional NPIs has an additional and not negligible effect, which is easily concluded from the difference between the results of simulation 3 and the actual observed situation.

These results jointly with the results of the impact of the NPIs above suggest the joint effect of *Facial coverings* and *Workplace closing* is major among all the NPI combinations. Simulation 4 (one denotes it as *Facial coverings(-), Workplace closing(+)*) considers the situation where only the effects of facial covers on the probability of transmission and the two *Workplace closing* stringency levels on the contact-mobility levels are accounted for. It is clear from the results reported in Table 5 and illustrated in Figures A5, A6 and A7 that even adopting only these two NPIs together would have resulted in posteponing the peak of the incidence (see Figure A6), and in a number of infections hardly managed by the National Health System. Indeed, by December 26^{th} the number of accumulated infections, the accumulated deaths, and and the maximum of daily infections would have reached 7.1 million, 59.8 thousand, and 75.7 thousand, respectively. It is even possible to support the statement that the sooner enforcement of wearing face mask (the use of facial masks became required only on October 28^{th} 2020) would have been positive both for incidence of infections and deaths, but not sufficient to avoid an unmanageable burden in the health system.

4 Discussion and future work

In this work, the main classes of public health measures that aim to prevent and/or control infection transmission in the community were characterised and presented under a common umbrella named Non-Pharmaceutical Interventions (NPIs). In particular, those put into force in Portugal were considered. Ultimately, the scientific community and government officials need proof of their effectiveness in reducing the number of contacts between individuals, specially between the most exposed to infection and those who present particular vulnerabilities, and therefore mitigate and contain the spread of the infection. This proof is even more critical when there was no effective and safe vaccine to protect those at risk of severe COVID-19, NPIs were seen as the most effective measures against COVID-19. As the social and economic costs may vary significantly between NPI measures, it is of utmost importance to offer some insight into the ones that may be more effective in preventing the spread of the disease. The reduction of individual contacts is hard to quantify, but proxy variables exist that aid in the investigation of NPI effects, having the mobility information widely available on the Internet as an example of a potential proxy.

A SEIRD model was fitted to the COVID-19 epidemic data of Portugal to achieve this primary objective. The model was estimated through a Bayesian hierarchical framework and a set of singular model features used to assess the role of mobility data as a potential proxy of the reduction of individual contacts. Furthermore, once the critical role of mobility data was established, several other issues were investigated, namely the quantification of the impact of those NPIs on the course of the epidemic curves. The methodology presented in this work might be even extended for other purposes such as simulation of the effect of specific interventions.

The age-structured SEIRD model framework considered the generation of daily infections to be a function of the virus-inherent probability of transmission and the contact rate - the number of people an average person entered into contact with on a daily basis. We considered the contact rates to be heterogeneous across age-groups. A matrix of average daily prior pandemic contacts per age-group is used. It is supposed to evolve according to a corresponding mobility index computed using Google mobility data. A full contact-mobility matrix resulted and is used to mimic the temporal path of mixing pattern. The contact-mobility matrix entries are considered stochastic and assumed to vary according to the impact of the NPIs.

Assuming a constant virus-inherent probability of transmission, which is not a hard assumption given the short period of analysis (the period prior to the vaccination phase which corresponds to the first 300 days of the pandemic in Portugal), the model fit is considered fair. Indeed, the visual fit is from Figures A1, A2, in the Appendix, regarding the age-group data, and Figures 6, 7 and 8 for all ages, depicting the observed and fitted number of accumulated and daily number of infected cases, accumulated deaths and recoveries, for the period corresponding to the used data. Indeed, the fitted number of accumulated infected cases underestimates the

observed value by 1.9% and the fitted number of accumulated deaths for the same period overestimates the observed value by 0.07%.

Given the unreliable nature of the data on daily recoveries, the fitted model considers the curve of recoveries a function of a constant and widely accepted recovery rate. Under this circumstance one would have necessarily expected a departure between the observed and estimated curves of recoveries. It was the case, which suggests a conservative approach by the public health authorities in the criteria to consider an infected individual not infectious any more.

Regarding the contact-mobility matrix, another target of the proposed model, the fit fair as well. Indeed, on one hand the baseline prior pandemic contact matrix is accurately reproduced (Figure A4), and on the other, the main festures of its temporal path, represented by the summary mobility index, are fairly fitted (Figures A3)

The age-group fatality rates, μ_i,$i = 1, ..., 8$, are not significantly different from zero (at 5% significance level) for the first two age-groups, [0,9] and [10,19] years of age. For the remaining age-groups, fatality rates are statistically significant, but still not different from zero in practical terms. The last age group is where fatality concentrate the most.

The baseline probability that a contact provokes the transmission of the disease is, under the model, highly low, around 0.25%. However, the risk of a contact provoking the transmission of the disease suffers a reduction of 40.2%, when facial coverings became *required in **some** specified shared/public spaces outside the home with other people present, or **some** situations when social distancing was not possible*. Moreover, when the stringency of this NPI increased, that is, when facial covering became *required in **all** shared/public spaces outside the home with other people present or **all** situations when social distancing was not possible* the risk dropped even sharper by 59.0%. Although, these two effects are statistically significant, they had a moderate impact in the course of the pandemic. In fact, the comparison between simulations shows the impact of using facial covering is much lower than the effect of all other NPIs in lowering contacts between individuals.

Among the other NPIs, the crucial contributions to the reduction of the prior pandemic contact levels and therefore to the spread of infection must be emphasised, were by the following order of importance *Workplace closing*, *Stay at home requirements* (lockdown) and *Restrictions on internal movement*. These results are, in general, in line with what has been published in the literature (e.g. Mendez-Brito et al. (2021)). The lockdown intervention impact on the number of infections cannot be measured directly. However, results confirm the growth of the contact-mobility mixing in residential areas, certainly reducing the mixing in places where the infection would have spread out easily. Works exist reporting the importance of *School closing* as a mean of reducing the spread of the infection (cf. Section 1). These results are fully understandable, given the mixing of students within schools and their families. However, as we do not have data on infections by source of infection it turns hard to assess

this effect. Moreover, the results reported here do not support this thesis.

In short, the results obtained here are fourfold. Firstly, thanks to the universal wearing of facial coverings, the probability that a contact provoked the transmission of the disease was reduced by more than 50%. Secondly, the impact of the other NPI (from which *Workplace closing* stands clearly out) is so significant that otherwise Portugal would have gone into a non-sustainable situation of having 80% of its population infected in the first 300 days of the pandemic. This situation would have led to a number of deaths more than twenty times higher than the number that was actually recorded by December 26^{th}, 2020. Thirdly, the requirement of wearing face masks and working-from-home (*Workplace closing*) whenever possible had a impact on reducing the probability of transmission and preventing physical contacts among the population that would not have been sufficient for Portugal to avoid an unmanageable number of infection. Therefore, the it seems clear the the economic and social effects of NPIs adopted could not have been avoided. And lastly, the observed curve of recovery cases in Portugal suggests health authorities followed a conservative approach on the criteria to consider an infected individual not infectious any longer.

This work is clearly limited by the unavailability of data on infections by source of infection and mobility data stratified by age-group. This lack of data prevented the authors to go deeper in the consideration of different contact matrices according to the place where infections occurred and forced them to use of a mobility index uniform across all age-groups. Consideration of these data would have turned possible modelling accurately some sources of heterogeneity. Moreover, the modelling approach does not consider the impact in a more extended period as the vaccination effect was not considered. Including the effect of the vaccination in the burden caused to the health system should be a priority in the near future. These implies extending the analysis to the year of 2021, where the hardest wave of infections hit the country, requiring (1) the consideration of other model compartments, as suggested by Mendes and Coelho (2021), and (2) the incorporation of effects of different SARS-Cov-2 variants on the probability of transmission and morbidity.

5 References

Abou-Ismail, Anas. 2020. "Compartmental Models of the COVID-19 Pandemic for Physicians and Physician-Scientists." *SN Comprehensive Clinical Medicine* 2. doi: 10.1007/s42399-020-00330-z.

Anderson, Roy M. 1991. "Discussion: The Kermack-McKendrick Epidemic Threshold Theorem." *Bulletin of Mathematical Biology* 53. doi: 10.1007/BF02464422.

Arregui, Sergio, Alberto Aleta, Joaquín Sanz, and Yamir Moreno. 2018. "Projecting Social Contact Matrices to Different Demographic Structures." *PLoS Computational Biology* 14. doi: 10.1371/journal.pcbi.1006638.

Banholzer, Nicolas, Adrian Lison, Dennis Ozcelik, Tanja Stadler, Stefan Feuerriegel, and Werner Vach. 2022. "The Methodologies to Assess the Effectiveness of Non-Pharmaceutical Interventions During COVID-19: A Systematic Review." *EUROPEAN JOURNAL OF EPIDEMIOLOGY* 37(10):1003–24. doi: 10.1007/s10654-022-00908-y.

Banholzer, Nicolas, Eva Van Weenen, Adrian Lison, Alberto Cenedese, Arne Seeliger, Bernhard Kratzwald, Daniel Tschernutter, Joan Puig Salles, Pierluigi Bottrighi, Sonja Lehtinen, Stefan Feuerriegel, and Werner Vach. 2021. "Estimating the Effects of Non-Pharmaceutical Interventions on the Number of New Infections with COVID-19 During the First Epidemic Wave." *PLoS ONE* 16. doi: 10.1371/journal.pone.0252827.

Barbarossa, Maria Vittoria, and Jan Fuhrmann. 2021. "Compliance with NPIs and Possible Deleterious Effects on Mitigation of an Epidemic Outbreak." *INFECTIOUS DISEASE MODELLING* 6:859–74. doi: 10.1016/j.idm.2021.06.001.

Brauner, Jan M., Sören Mindermann, Mrinank Sharma, David Johnston, John Salvatier, Tomáš Gavenčiak, Anna B. Stephenson, Gavin Leech, George Altman, Vladimir Mikulik, Alexander John Norman, Joshua Teperowski Monrad, Tamay Besiroglu, Hong Ge, Meghan A. Hartwick, Yee Whye Teh, Leonid Chindelevitch, Yarin Gal, and Jan Kulveit. 2021. "Inferring the Effectiveness of Government Interventions Against COVID-19." *Science* 371. doi: 10.1126/science.abd9338.

Brooks, Stephen P., and Andrew Gelman. 1998. "General Methods for Monitoring Convergence of Iterative Simulations)?" *Journal of Computational and Graphical Statistics* 7. doi: 10.1080/10618600.1998.10474787.

Chan, Jasper Fuk Woo, Shuofeng Yuan, Kin Hang Kok, Kelvin Kai Wang To, Hin Chu, Jin Yang, Fanfan Xing, Jieling Liu, Cyril Chik Yan Yip, Rosana Wing Shan Poon, Hoi Wah Tsoi, Simon Kam Fai Lo, Kwok Hung Chan, Vincent Kwok Man Poon, Wan Mui Chan, Jonathan Daniel Ip, Jian Piao Cai, Vincent Chi Chung Cheng, Honglin Chen, Christopher Kim Ming Hui, and Kwok Yung Yuen. 2020. "A Familial Cluster of Pneumonia Associated with the 2019 Novel Coronavirus Indicating Person-to-Person Transmission: A Study of a Family Cluster." *The Lancet* 395. doi: 10.1016/S0140-6736(20)30154-9.

Chen, Jieliang. 2020. "Pathogenicity and Transmissibility of 2019-nCoV—a Quick Overview and Comparison with Other Emerging Viruses." *Microbes and Infection* 22. doi: 10.1016/j.micinf.2020.01.004.

Chikina, Maria, and Wesley Pegden. 2020. "Modeling Strict Age-Targeted Mitigation Strategies for COVID-19" edited by L. A. Braunstein. *PLOS ONE* 15:e0236237. doi: 10.1371/journal.pone.0236237.

Diekmann, O., J. A. P. Heesterbeek, and J. A. J. Metz. 1990. "On the Definition and the Computation of the Basic Reproduction Ratio R0 in Models for Infectious Diseases in Heterogeneous Populations." *Journal of Mathematical Biology* 28. doi: 10.1007/BF00178324.

Disease Prevention, European Center for, and Control. 2020. "Outbreak of Novel Coronavirus Disease 2019 (COVID-19): Increased Transmission Globally – Fifth Update." *Rapid Risk Assessment* 2019.

Disease Prevention, European Centre for, and Control. 2020. "Guidelines for Non-Pharmaceutical Interventions to Reduce the Impact of COVID-19 in the EU/EEA and the UK."

Downing, Seth T., Ryan J. Mccarty, Andrea D. Guastello, Danielle L. Cooke, and Joseph P. H. Mcnamara. 2022. "Assessing the Predictors of Adaptive and Maladaptive Covid-19 Preventive Behaviours: An Application of Protection Motivation Theory." *PSYCHOLOGY HEALTH & MEDICINE*. doi: 10.1080/13548506.2022.2093925.

DSSG. 2022. "Covid19pt-Data." *Https://Raw.githubusercontent.com/Dssg-Pt/Covid19pt-Data/Master/Data.csv, Accessed: 2022-05-26.*

Eikenberry, Steffen E., Marina Mancuso, Enahoro Iboi, Tin Phan, Keenan Eikenberry, Yang Kuang, Eric Kostelich, and Abba B. Gumel. 2020. "To Mask or Not to Mask: Modeling the Potential for Face Mask Use by the General Public to Curtail the COVID-19 Pandemic." *Infectious Disease Modelling* 5. doi: 10.1016/j.idm.2020.04.001.

Ferguson, Neil M., Laydon Daniel, Nedjati-Gilani Gemma, Imai Natsuko, Kylie Ainslie, Baguelin Marc, Bhatia Sangeeta, Boonyasiri Adhiratha, Cucunubá Zulma, Cuomo-Dannenburg Gina, Dighe Amy, Dorigatti Ilaria, Fu Han, Gaythorpe Katy, Green Will, Hamlet Arran, Hinsley Wes, Lucy C. Okell, van Elsland Sabine, Thompson Hayley, Verity Robert, Volz Erik, Wang Haowei, Wang Yuanrong, Walker Patrick GT, Walters Caroline, Winskill Peter, Whittaker Charles, Donnelly Christl A, Riley Steven, and Ghani Azra C. 2020. "Impact of Non-Pharmaceutical Interventions (NPIs) to Reduce COVID-19 Mortality and Healthcare Demand." *Imperial College COVID-19 Response Team.* doi: https://doi.org/10.25561/77482.

Gilks, R., Sylvia Richardson, and David J. Spiegelhalter. 1996. *Markov Chain Monte Carlo in Practice: Interdisciplinary Statistics.*

Godio, Alberto, Francesca Pace, and Andrea Vergnano. 2020. "Seir Modeling of the Italian Epidemic of Sars-Cov-2 Using Computational Swarm Intelligence." *International Journal of Environmental Research and Public Health* 17. doi: 10.3390/ijerph17103535.

Gozzi, Nicolò, Paolo Bajardi, and Nicola Perra. 2021. "The Importance of Non-Pharmaceutical Interventions During the COVID-19 Vaccine Rollout." *PLoS Computational Biology* 17. doi: 10.1371/journal.pcbi.1009346.

Haug, Nils, Lukas Geyrhofer, Alessandro Londei, Elma Dervic, Amélie Desvars-Larrive, Vittorio Loreto, Beate Pinior, Stefan Thurner, and Peter Klimek. 2020. "Ranking

the Effectiveness of Worldwide COVID-19 Government Interventions." *Nature Human Behaviour* 4. doi: 10.1038/s41562-020-01009-0.

Hengartner, Michael P., Gregor Waller, and Agnes von Wyl. 2022. "Factors Related to Non-Compliance with Non-Pharmaceutical Interventions to Mitigate the Spread of SARS-CoV-2: Results from a Survey in the Swiss General Adult Population." *FRONTIERS IN PUBLIC HEALTH* 10. doi: 10.3389/fpubh.2022.828584.

Hethcote, Herbert W. 2000. "Mathematics of Infectious Diseases." *SIAM Review* 42. doi: 10.1137/S0036144500371907.

Kaye, Paul M. 1993. "Infectious Diseases of Humans: Dynamics and Control. Roy m. Anderson and Robert m. May, Oxford University Press, 1992. £22.50 (Viii + 757 Pages) ISBN 0 19 854040 x." *Immunology Today* 14. doi: 10.1016/0167-5699(93)90204-X.

Kermack, W. O., and A. G. McKendrick. 1927. "A Contribution to the Mathematical Theory of Epidemics." *Proceedings of the Royal Society of London. Series A, Containing Papers of a Mathematical and Physical Character* 115. doi: 10.1098/rspa.1927.0118.

Kretzschmar, Mirjam E., Ben Ashby, Elizabeth Fearon, Christopher E. Overton, Jasmina Panovska-Griffiths, Lorenzo Pellis, Matthew Quaife, Ganna Rozhnova, Francesca Scarabel, Helena B. Stage, Ben Swallow, Robin N. Thompson, Michael J. Tildesley, and Daniel Villela. 2022. "Challenges for Modelling Interventions for Future Pandemics." *EPIDEMICS* 38. doi: 10.1016/j.epidem.2022.100546.

Lauer, Stephen A., Kyra H. Grantz, Qifang Bi, Forrest K. Jones, Qulu Zheng, Hannah R. Meredith, Andrew S. Azman, Nicholas G. Reich, and Justin Lessler. 2020. "The Incubation Period of Coronavirus Disease 2019 (CoVID-19) from Publicly Reported Confirmed Cases: Estimation and Application." *Annals of Internal Medicine* 172. doi: 10.7326/M20-0504.

Leech, Gavin, Charlie Rogers-Smith, Joshua Teperowski Monrad, Jonas B. Sandbrink, Benedict Snodin, Robert Zinkov, Benjamin Rader, John S. Brownstein, Yarin Gal, Samir Bhatt, Mrinank Sharma, Sören Mindermann, Jan M. Brauner, and Laurence Aitchison. 2022. "Mask Wearing in Community Settings Reduces SARS-CoV-2 Transmission." *Proceedings of the National Academy of Sciences* 119(23):e2119266119. doi: 10.1073/pnas.2119266119.

Li, Qun, Xuhua Guan, Peng Wu, Xiaoye Wang, Lei Zhou, Yeqing Tong, Ruiqi Ren, Kathy S. M. Leung, Eric H. Y. Lau, Jessica Y. Wong, Xuesen Xing, Nijuan Xiang, Yang Wu, Chao Li, Qi Chen, Dan Li, Tian Liu, Jing Zhao, Man Liu, Wenxiao Tu, Chuding Chen, Lianmei Jin, Rui Yang, Qi Wang, Suhua Zhou, Rui Wang, Hui Liu, Yinbo Luo, Yuan Liu, Ge Shao, Huan Li, Zhongfa Tao, Yang Yang, Zhiqiang Deng, Boxi Liu, Zhitao Ma, Yanping Zhang, Guoqing Shi, Tommy T. Y. Lam, Joseph T. Wu, George F. Gao, Benjamin J. Cowling, Bo Yang, Gabriel M. Leung, and Zijian Feng. 2020. "Early Transmission Dynamics in Wuhan, China, of Novel Coronavirus–Infected Pneumonia." *New England Journal of Medicine* 382. doi: 10.1056/nejmoa2001316.

Linton, Natalie M., Tetsuro Kobayashi, Yichi Yang, Katsuma Hayashi, Andrei R. Akhmetzhanov, Sung-mok Jung, Baoyin Yuan, Ryo Kinoshita, and Hiroshi Nishiura. 2020. "Epidemiological Characteristics of Novel Coronavirus Infection: A Statistical Analysis of

Publicly Available Case Data." *medRxiv*. doi: 10.1101/2020.01.26.20018754.

Liu, Yang, Christian Morgenstern, James Kelly, Rachel Lowe, James Munday, C. Julian Villabona-Arenas, Hamish Gibbs, Carl A. B. Pearson, Kiesha Prem, Quentin J. Leclerc, Sophie R. Meakin, W. John Edmunds, Christopher I. Jarvis, Amy Gimma, Sebastian Funk, Matthew Quaife, Timothy W. Russell, Jon C. Emory, Sam Abbott, Joel Hellewell, Damien C. Tully, Rein M. G. J. Houben, Kathleen O'Reilly, Georgia R. Gore-Langton, Adam J. Kucharski, Megan Auzenbergs, Billy J. Quilty, Thibaut Jombart, Alicia Rosello, Oliver Brady, Katherine E. Atkins, Kevin van Zandvoort, James W. Rudge, Akira Endo, Kaja Abbas, Fiona Yueqian Sun, Simon R. Procter, Samuel Clifford, Anna M. Foss, Nicholas G. Davies, Yung Wai Desmond Chan, Charlie Diamond, Rosanna C. Barnard, Rosalind M. Eggo, Arminder K. Deol, Emily S. Nightingale, David Simons, Katharine Sherratt, Graham Medley, Stéphane Hué, Gwenan M. Knight, Stefan Flasche, Nikos I. Bosse, Petra Klepac, and Mark Jit. 2021. "The Impact of Non-Pharmaceutical Interventions on SARS-CoV-2 Transmission Across 130 Countries and Territories." *BMC Medicine* 19. doi: 10.1186/s12916-020-01872-8.

Mendes, Jorge M., and Pedro S. Coelho. 2021. "Addressing Hospitalisations with Non-Error-Free Data by Generalised SEIR Modelling of COVID-19 Pandemic." *Scientific Reports* 11. doi: 10.1038/s41598-021-98975-w.

Mendez-Brito, Alba, Charbel El Bcheraoui, and Francisco Pozo-Martin. 2021. "Systematic Review of Empirical Studies Comparing the Effectiveness of Non-Pharmaceutical Interventions Against COVID-19." *Journal of Infection* 83.

Moher, David, Alessandro Liberati, Jennifer Tetzlaff, Douglas G. Altman, Doug Altman, Gerd Antes, David Atkins, Virginia Barbour, Nick Barrowman, Jesse A. Berlin, Jocalyn Clark, Mike Clarke, Deborah Cook, Roberto D'Amico, Jonathan J. Deeks, P. J. Devereaux, Kay Dickersin, Matthias Egger, Edzard Ernst, Peter C. Gøtzsche, Jeremy Grimshaw, Gordon Guyatt, Julian Higgins, John P. A. Ioannidis, Jos Kleijnen, Tom Lang, Nicola Magrini, David McNamee, Lorenzo Moja, Cynthia Mulrow, Maryann Napoli, Andy Oxman, Bá Pham, Drummond Rennie, Margaret Sampson, Kenneth F. Schulz, Paul G. Shekelle, David Tovey, and Peter Tugwell. 2009. "Preferred Reporting Items for Systematic Reviews and Meta-Analyses: The PRISMA Statement." *PLoS Medicine* 6. doi: 10.1371/journal.pmed.1000097.

Mossong, Niel AND Jit, Joël AND Hens. 2008. "Social Contacts and Mixing Patterns Relevant to the Spread of Infectious Diseases." *PLOS Medicine* 5(3):1–1. doi: 10.1371/journal.pmed.0050074.

Ndaïrou, Faïçal, Iván Area, Georg Bader, Juan J. Nieto, and Delfim F. M. Torres. 2020. "Corrigendum to 'Mathematical Modeling of COVID-19 Transmission Dynamics with a Case Study of Wuhan' [Chaos Solitons Fractals 135 (2020), 109846] (Chaos, Solitons & Fractals (2020) 135(109846), (10.1016/j.chaos.2020.109846))." *Chaos, Solitons and Fractals* 141.

Nunan, D., and J. Brassey. 2020. "What Is the Evidence for Mass Gatherings During Global Pandemics?" *The Centre for Evidence Based Medicine*.

Prem, Kiesha, Alex R. Cook, and Mark Jit. 2017. "Projecting Social Contact Matrices in 152 Countries Using Contact Surveys and Demographic Data." *PLoS Computational Biology* 13. doi: 10.1371/journal.pcbi.1005697.

Ram, Vishaal, and Laura P. Schaposnik. 2021. "A Modified Age-Structured SIR Model for COVID-19 Type Viruses." *Scientific Reports* 11. doi: 10.1038/s41598-021-94609-3.

Rosa, Giuseppina La, Lucia Bonadonna, Luca Lucentini, Sebastien Kenmoe, and Elisabetta Suffredini. 2020. "Coronavirus in Water Environments: Occurrence, Persistence and Concentration Methods - a Scoping Review." *Water Research* 179. doi: 10.1016/j.watres.2020.115899.

Santos, Joao Vasco, Joana Gomes da Costa, Eduardo Costa, Sara Almeida, Joana Cima, and Pedro Pita-Barros. 2022. "Factors Associated with Non-Pharmaceutical Interventions Compliance During COVID-19 Pandemic: A Portuguese Cross-Sectional Survey." *JOURNAL OF PUBLIC HEALTH*. doi: 10.1093/pubmed/fdac001.

Seale, Holly, Clare E. F. Dyer, Ikram Abdi, Kazi M. Rahman, Yanni Sun, Mohammed O. Qureshi, Alexander Dowell-Day, Jonathon Sward, and M. Saiful Islam. 2020. "Improving the Impact of Non-Pharmaceutical Interventions During COVID-19: Examining the Factors That Influence Engagement and the Impact on Individuals." *BMC INFECTIOUS DISEASES* 20(1). doi: 10.1186/s12879-020-05340-9.

Shittu, Ekundayo, Funmilayo Adewumi, Nkemdilim Ene, Somto Chloe Keluo-Udeke, and Chizoba Wonodi. 2022. "Examining Psychosocial Factors and Community Mitigation Practices to Limit the Spread of COVID-19: Evidence from Nigeria." *HEALTHCARE* 10(3). doi: 10.3390/healthcare10030585.

Snoeijer, Berber T., Mariska Burger, Shaoxiong Sun, Richard J. B. Dobson, and Amos A. Folarin. 2021. "Measuring the Effect of Non-Pharmaceutical Interventions (NPIs) on Mobility During the COVID-19 Pandemic Using Global Mobility Data." *Npj Digital Medicine* 4. doi: 10.1038/s41746-021-00451-2.

Sopory, Pradeep, Julie M. Novak, and Jane P. Noyes. 2022. "Quarantine Acceptance and Adherence: Qualitative Evidence Synthesis and Conceptual Framework." *JOURNAL OF PUBLIC HEALTH-HEIDELBERG* 30(9):2091–101. doi: 10.1007/s10389-021-01544-8.

Suryanarayanan, Parthasarathy, Ching Huei Tsou, Ananya Poddar, Diwakar Mahajan, Bharath Dandala, Piyush Madan, Anshul Agrawal, Charles Wachira, Osebe Mogaka Samuel, Osnat Bar-Shira, Clifton Kipchirchir, Sharon Okwako, William Ogallo, Fred Otieno, Timothy Nyota, Fiona Matu, Vesna Resende Barros, Daniel Shats, Oren Kagan, Sekou Remy, Oliver Bent, Pooja Guhan, Shilpa Mahatma, Aisha Walcott-Bryant, Divya Pathak, and Michal Rosen-Zvi. 2021. "AI-Assisted Tracking of Worldwide Non-Pharmaceutical Interventions for COVID-19." *Scientific Data* 8. doi: 10.1038/s41597-021-00878-y.

Tang, Biao, Nicola Luigi Bragazzi, Qian Li, Sanyi Tang, Yanni Xiao, and Jianhong Wu. 2020. "An Updated Estimation of the Risk of Transmission of the Novel Coronavirus (2019-nCov)." *Infectious Disease Modelling* 5. doi: 10.1016/j.idm.2020.02.001.

Wang, Kai, Zhenzhen Lu, Xiaomeng Wang, Hui Li, Huling Li, Dandan Lin, Yongli Cai,

Xing Feng, Yateng Song, Zhiwei Feng, Weidong Ji, Xiaoyan Wang, Yi Yin, Lei Wang, and Zhihang Peng. 2020. "Current Trends and Future Prediction of Novel Coronavirus Disease (COVID-19) Epidemic in China: A Dynamical Modeling Analysis." *Mathematical Biosciences and Engineering* 17. doi: 10.3934/MBE.2020173.

Zhou, Fei, Ting Yu, Ronghui Du, Guohui Fan, Ying Liu, Zhibo Liu, Jie Xiang, Yeming Wang, Bin Song, Xiaoying Gu, Lulu Guan, Yuan Wei, Hui Li, Xudong Wu, Jiuyang Xu, Shengjin Tu, Yi Zhang, Hua Chen, and Bin Cao. 2020. "Clinical Course and Risk Factors for Mortality of Adult Inpatients with COVID-19 in Wuhan, China: A Retrospective Cohort Study." *The Lancet* 395. doi: 10.1016/S0140-6736(20)30566-3.

Zhu, Na, Dingyu Zhang, Wenling Wang, Xingwang Li, Bo Yang, Jingdong Song, Xiang Zhao, Baoying Huang, Weifeng Shi, Roujian Lu, Peihua Niu, Faxian Zhan, Xuejun Ma, Dayan Wang, Wenbo Xu, Guizhen Wu, George F. Gao, and Wenjie Tan. 2020. "A Novel Coronavirus from Patients with Pneumonia in China, 2019." *New England Journal of Medicine* 382. doi: 10.1056/nejmoa2001017.

A Appendix

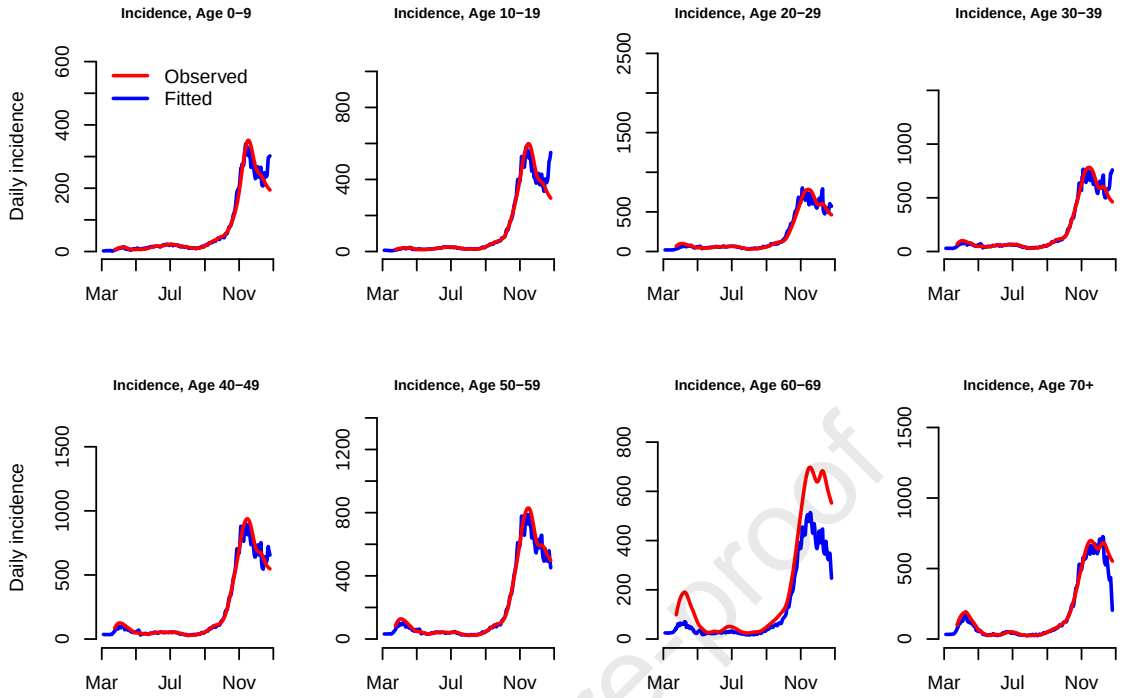

Figure A1: Model fitting - observed and fitted values. Observed daily confirmed cases of infection and means of posterior distributions of $dI_i(t)$, $i = 1, ..., 8$. Due to intra week variation observed values were smoothed using a gaussian kernel smoother with bandwidth 14 days.

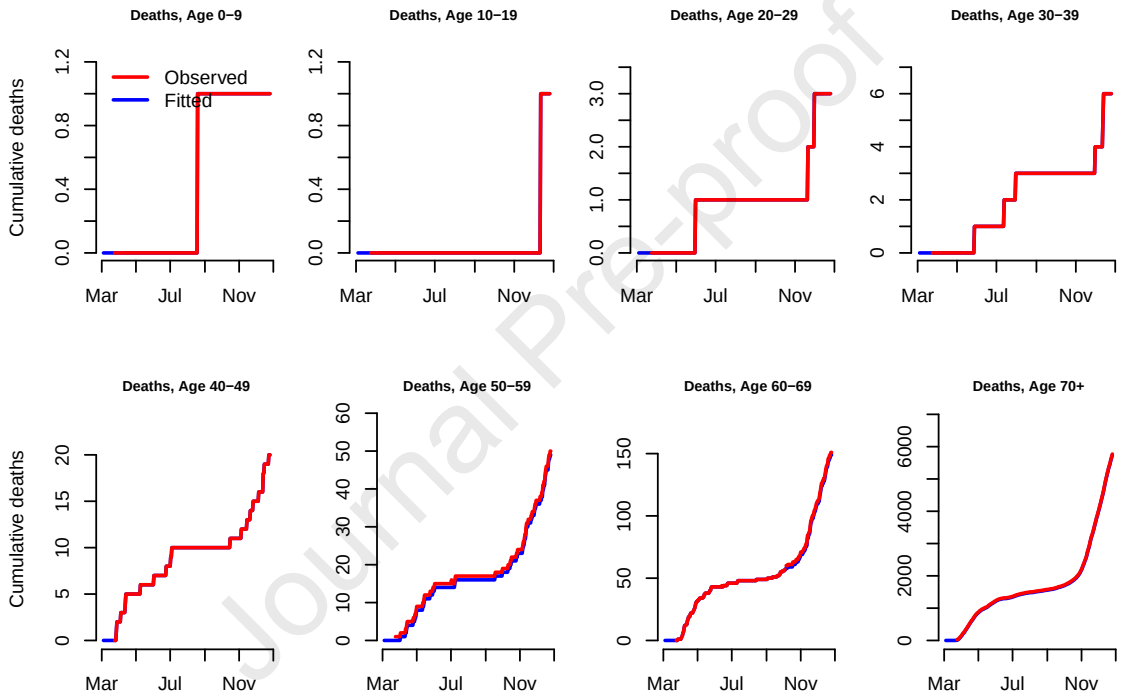

Figure A2: Model fitting - observed and fitted values. Observed daily accumulated deaths and means of posterior distribution of $D_i(t)$, $i = 1, ..., 8$.

Table A1: Non-pharmaceutical interventions considered in this work. More information can be found here https://www.bsg.ox.ac.uk/research/research-projects/covid-19-government-response-tracker and here https://www.bsg.ox.ac.uk/research/publications/variation-government-responses-covid-19

Name	Coding
(C1) School closing	0 - no measures 1 - recommend closing or all schools open with alterations resulting in significant differences compared to non-Covid-19 operations 2 - require closing (only some levels or categories, e.g. just high school, or just public schools) 3 - require closing all levels **Levels 1, 2 and 3 aggregated together**
(C2) Workplace closing	0 - no measures 1 - recommend closing (or recommend work from home) or all businesses open with alterations resulting in significant differences compared to non-Covid-19 operation 2 - require closing (or work from home) for some sectors or categories of workers 3 - require closing (or work from home) for all-but-essential workplaces (e.g. grocery stores, doctors) **Level 1 does not apply to Portugal**
(C3) Cancel public events	0 - no measures 1 - recommend cancelling 2 - require cancelling **Level 1 does not apply to Portugal**
(C4) Restrictions on gatherings	0 - no restrictions 1 - restrictions on very large gatherings (the limit is above 1000 people) 2 - restrictions on gatherings between 101-1000 people 3 - restrictions on gatherings between 11-100 people 4 - restrictions on gatherings of 10 people or less **Level 1 does not apply to Portugal. Levels 2, 3 and 4 aggregated together.**
(C5) Close public transport	0 - no measures 1 - recommend closing (or significantly reducing volume/route/means of transport available) 2 - require closing (or prohibit most citizens from using it) **Level 2 does not apply to Portugal.**
(C6) Stay at home requirements	0 - no measures 1 - recommend not leaving house 2 - require not leaving house with exceptions for daily exercise, grocery shopping, and 'essential' trips 3 - require not leaving house with minimal exceptions (e.g. allowed to leave once a week or only one person can leave at a time, etc) **Level 3 does not apply to Portugal.**
(C7) Restrictions on internal movement	0 - no measures 1 - recommend not to travel between regions/cities 2 - internal movement restrictions in place **Levels 1 and 2 aggregated together.**
(C8) International travel controls	0 - no restrictions 1 - screening arrivals 2 - quarantine arrivals from some or all regions 3 - ban arrivals from some regions 4 - ban on all regions or total border closure **Levels 1, 2 and 4 do not apply to Portugal**
(H6) Facial coverings	0 - No policy 1 - Recommended 2 - Required in some specified shared/public spaces outside the home with other people present or some situations when social distancing is not possible 3 - Required in all shared/public spaces outside the home with other people present or all situations when social distancing is not possible 4 - Required outside the home at all times regardless of location or presence of other people **Levels 1 and 4 do not apply to Portugal**

Table A2: Gelman and Rubin's statistic

Parameter	R	Parameter	R
μ^1	1.03	$\lambda^0_{2,6}$	1.05
μ^2	1.00	$\lambda^0_{2,7}$	1.05
μ^3	1.02	$\lambda^0_{2,8}$	1.04
μ^4	1.00	$\lambda^0_{3,3}$	1.01
μ^5	1.00	$\lambda^0_{3,4}$	1.06
μ^6	1.00	$\lambda^0_{3,5}$	1.06
μ^7	1.00	$\lambda^0_{3,6}$	1.05
μ^8	1.00	$\lambda^0_{3,7}$	1.06
ρ_μ	1.00	$\lambda^0_{3,8}$	1.04
η_0	1.02	$\lambda^0_{4,4}$	1.00
η_1	1.01	$\lambda^0_{4,5}$	1.03
η_2	1.02	$\lambda^0_{4,6}$	1.07
θ_1	0.99	$\lambda^0_{4,7}$	1.03
θ_2	1.00	$\lambda^0_{4,8}$	1.05
θ_3	1.01	$\lambda^0_{5,5}$	1.01
θ_4	1.01	$\lambda^0_{5,6}$	1.06
θ_5	1.00	$\lambda^0_{5,7}$	1.06
θ_6	1.00	$\lambda^0_{5,8}$	1.04
θ_7	1.01	$\lambda^0_{6,6}$	1.00
θ_8	1.54	$\lambda^0_{6,7}$	1.04
$\lambda^0_{1,1}$	1.00	$\lambda^0_{6,8}$	1.04
$\lambda^0_{1,2}$	1.06	$\lambda^0_{7,7}$	1.00
$\lambda^0_{1,3}$	1.03	$\lambda^0_{7,8}$	1.05
$\lambda^0_{1,4}$	1.03	$\lambda^0_{8,8}$	1.06
$\lambda^0_{1,5}$	1.05	λ_{C1_1}	1.06
$\lambda^0_{1,6}$	1.06	λ_{C2_1}	1.06
$\lambda^0_{1,7}$	1.02	λ_{C2_2}	1.08
$\lambda^0_{1,8}$	1.03	λ_{C4_1}	1.08
$\lambda^0_{2,2}$	1.01	λ_{C5_1}	1.00
$\lambda^0_{2,3}$	1.03	λ_{C6_1}	1.00
$\lambda^0_{2,4}$	1.05	λ_{C7_1}	1.00
$\lambda^0_{2,5}$	1.09		

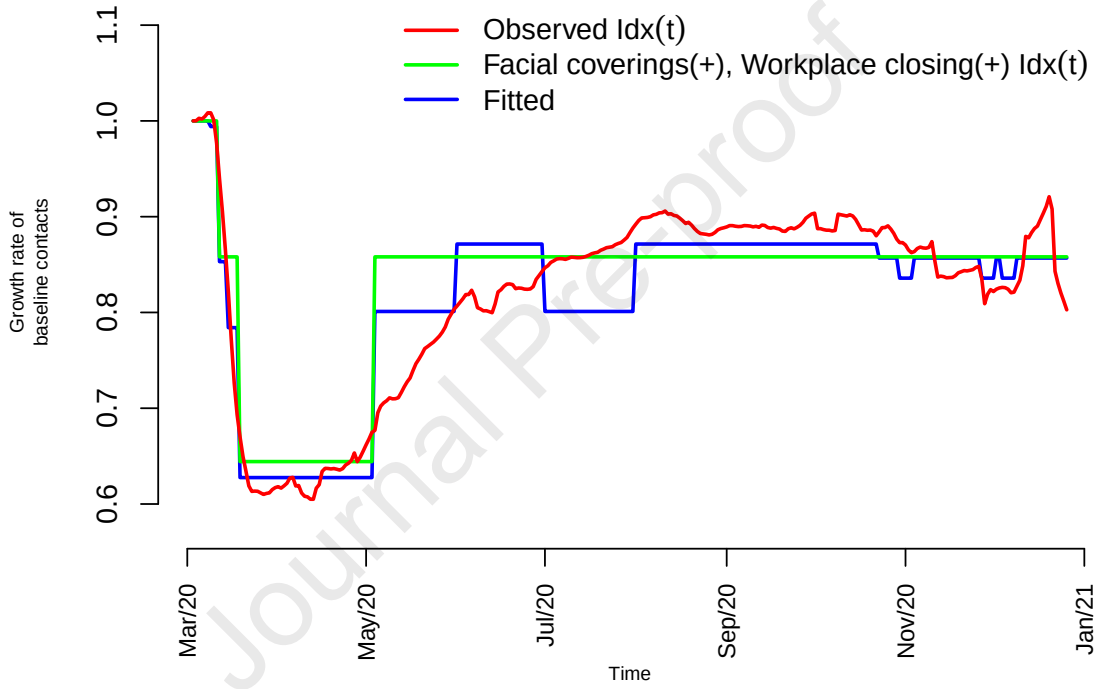

Figure A3: Model fitting results on the mobility matrix index, Idx(t). Lines represent the mean of the posterior distribution of $\exp(\boldsymbol{\lambda}\mathbf{X})$, in blue, (where $\mathbf{X}$ is the full matrix as in equation (21)), the mean of the posterior distribution of $\exp(\lambda^{C2_1}\mathrm{C2}_1(t) + \lambda^{C2_2}\mathrm{C2}_2(t))$, in green (corresponding to simulation 4 where only workplace closing and facial coverings are considered) and Idx(t) as defined in Section 2.2.3, in red.

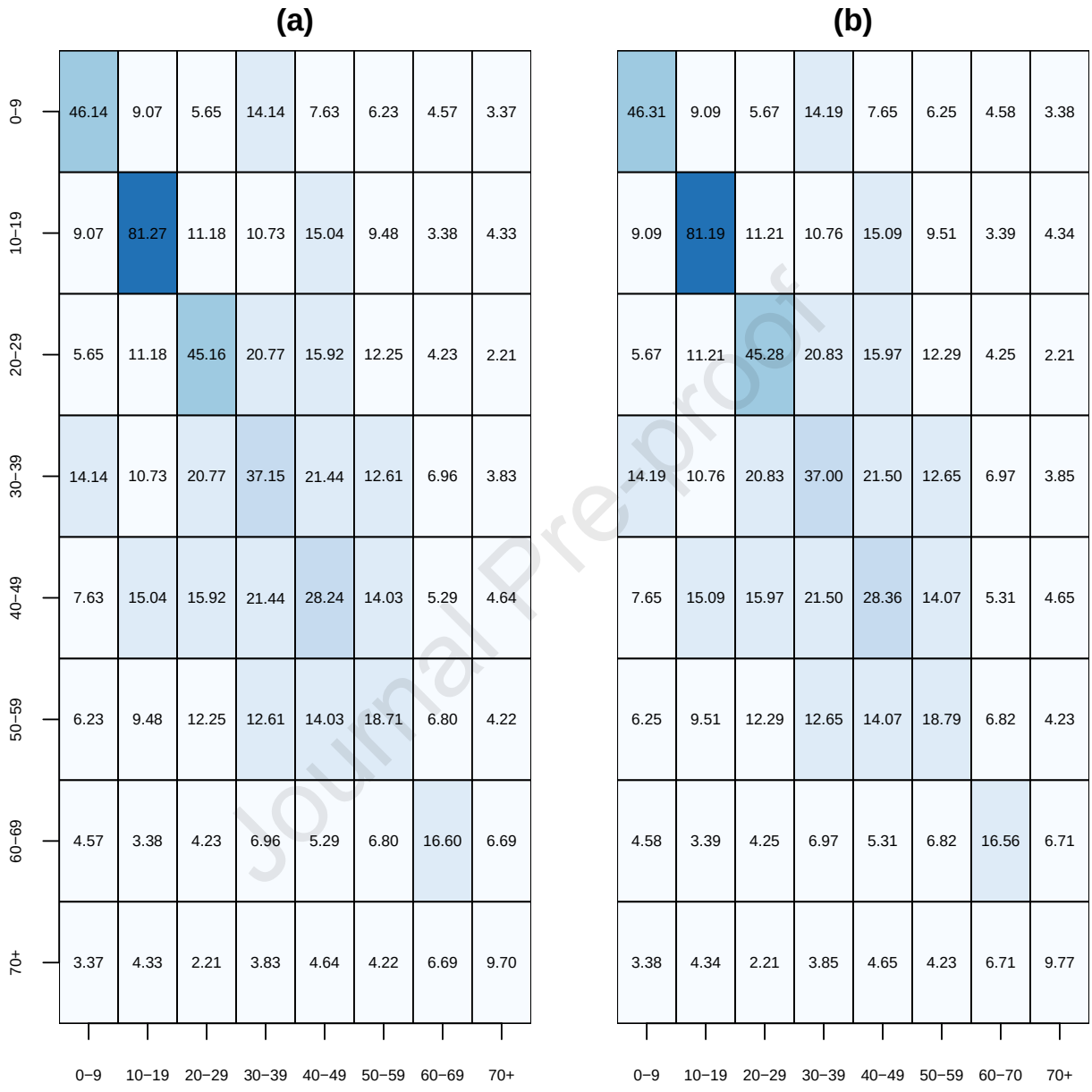

Figure A4: (a) Age-group baseline prior pandemic contact matrix $\mathbf{C}$ (Section 2.1.2) used in this work. Numbers represent the daily average number of contacts of people in the row age-group with people in the column age-group, and the 5-tone blue scale denotes their intensity. All ages are in years. (b) Results on the fitted contact matrix. The cell values correspond to mean of posterior distribution of $\exp(\lambda_{ij}^0)$, (see equation 21).

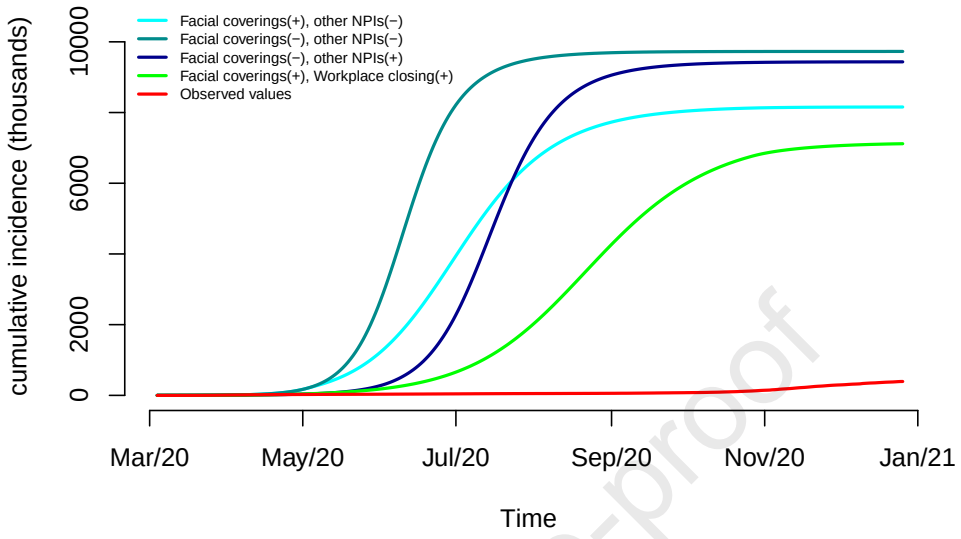

Figure A5: Results of simulations on observed cumulative incidence and simulated values (mean of the predictive distribution).

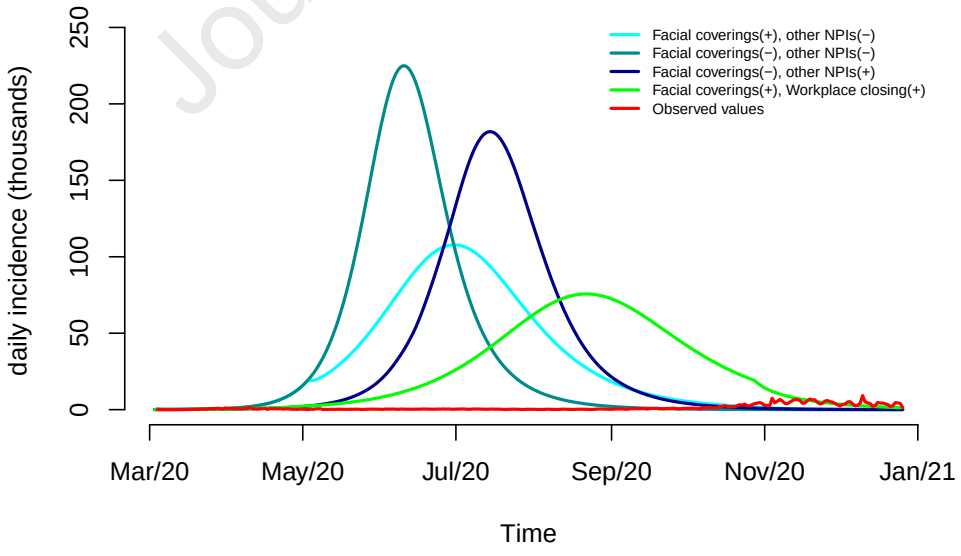

Figure A6: Results of simulations on observed daily incidence and simulated values (mean of the predictive distribution).

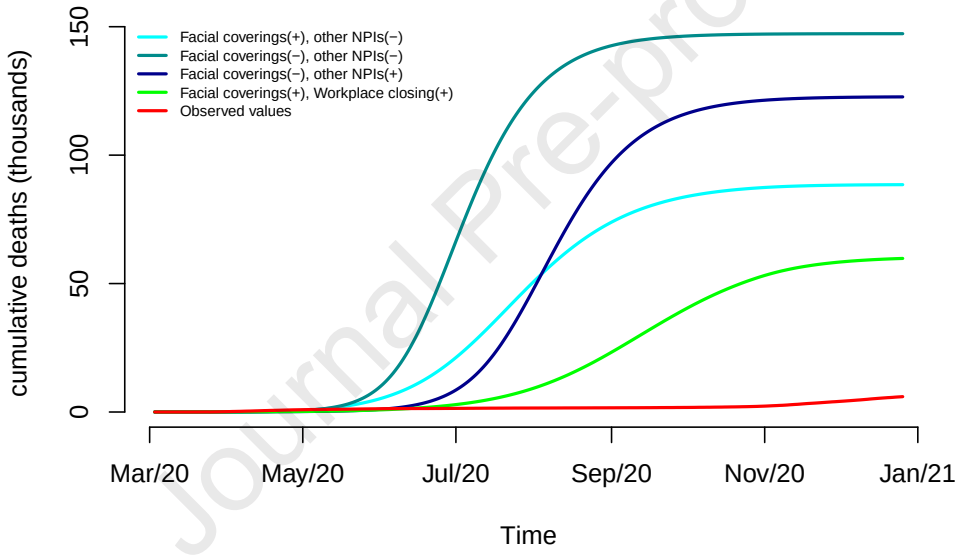

Figure A7: Results of simulations on observed accumulated deaths and simulated values (mean of the predictive distribution).

Declaration of interests

☒ The authors declare that they have no known competing financial interests or personal relationships that could have appeared to influence the work reported in this paper.

☐The authors declare the following financial interests/personal relationships which may be considered as potential competing interests:

Pedro Simões Coelho